Earth and Planetary Science Letters 331–332 (2012) 152–163

Contents lists available at SciVerse ScienceDirect

Earth and Planetary Science Letters

journal homepage: www.elsevier.com/locate/epsl

Late Cretaceous to recent plate motions in western South America revisited

Rubén Somoza [a,*], Marta E. Ghidella [b]

[a] IGEBA-CONICET, Departamento de Ciencias Geológicas, FCEyN, Universidad de Buenos Aires, Buenos Aires, Argentina
[b] Instituto Antártico Argentino, Buenos Aires, Argentina

ARTICLE INFO

Article history:
Received 29 April 2011
Received in revised form 24 January 2012
Accepted 2 March 2012
Available online xxxx

Editor: P. DeMenocal

Keywords:
Convergence
Andes
Late Cretaceous
Cenozoic

ABSTRACT

The Andean Cordillera has evolved since the Late Cretaceous in the context of subduction of oceanic lithosphere beneath continental lithosphere, making the kinematics between South America and its adjacent oceanic plates in the Pacific basin valuable to analyze the development of the Andean orogen. The latest Cretaceous–Cenozoic convergence history in western South America may be divided into three stages. The youngest Stage 1 (25–0 Ma) is characterized by ENE directed convergence of the Nazca plate toward most of South America, and by ~E–W subduction of the Antarctic plate beneath southern Patagonia. The Nazca–South America convergence rate in Stage 1 shows a continuous decrease from the highest values in the Cenozoic (~15 cm/yr) to the present day values from GPS measurements (~7 cm/yr). Stage 2 (47–28 Ma) is characterized by NE directed subduction of Farallon with the convergence rate remaining almost constant during the entire interval. In those times obliquity was dextral in Chile, sinistral in southern Peru, while almost head-on convergence occurred in central and northern Peru. During latest Cretaceous to Early Eocene times (Stage 3) the Farallon plate was subducted beneath Perú and the Phoenix plate was subducted farther south, where a triple junction migrated southward along the Chilean margin. The subduction of the Farallon plate was rather slow with variable direction imposed by the position of the triple junction, whereas subduction of the Phoenix plate was rapid (>10 cm/yr) and ESE directed. We present a working hypothesis suggesting no major changes in the age of subducted lithosphere in the Chile trench from Middle Eocene to Late Oligocene, followed by subduction of progressively older oceanic lithosphere in the early Neogene and progressively younger lithosphere during the late Neogene and the Quaternary. In addition, it is shown that South American motion as predicted by available hotspot models has insufficient resolution to be applied to the analysis of Cenozoic Andean deformation.

1. Introduction

The magmatic arc that parallels the western margin of South America has been almost permanently active since at least the Early Jurassic, indicating a long-lived subduction history. The coeval evolution of the continental margin may be divided into two periods. During Jurassic-Early Cretaceous times most of the margin was very close to sea level, with back-arc shallow seas and extensional basins. In contrast, the Late Cretaceous to Recent interval is distinguished by rising of arc massifs and predominance of horizontal shortening, leading to progressive crustal thickening, uplift, development of thrust belts and associated foreland basins. In the northern and southernmost Andes, some of the tectonic activity from this last evolutionary period is related to marginal basin closure and island arc accretion during the Late Cretaceous and Paleogene (e.g. Aleman and Ramos, 2000; Dalziel, 1981; Feininger and Bristow, 1980; Mégard, 1987). In contrast, the central Andean segment from ca 4° S to ca 45° S evolved in absence of collisions, involving autochthonous back-arc and magmatic arc rocks (Mégard, 1987; Mpodozis and Ramos, 1990; Ramos and Aleman, 2000), a scenario that also characterizes the Eocene to Recent evolution of the northern and southernmost Andes. These characteristics led to the consideration of the Andean cordillera as the type example of noncollisional orogen, formed in the context of convergence between oceanic and continental lithospheres (Dewey and Bird, 1970). Thus, Late Cretaceous to Recent relative motion between South America and its adjacent oceanic plates in the Pacific basin constitutes valuable information to analyze the development of the Andean orogen.

The last decade has seen the publication of many new findings and ideas concerning first order features in the Cenozoic Andes, such as the amount and timing of horizontal crustal-shortening, origin of crustal thickness, origin and timing of uplift of the Central Andean Plateau; shallowing of Wadati–Benioff zones; Cenozoic climate–tectonics interactions; and others (e.g. Ghiglione et al., 2010; Hampel, 2002; Hartley, 2003; Iaffaldano et al., 2006; Lamb and Davis, 2003; Liu et al., 2003; Martinod et al., 2010; McQuarrie, 2002; Müller et al., 2002; Schellart, 2008; Sobolev and Babeyko, 2005; Tassara et al., 2006; Yañez and Cembrano, 2004). Both relative plate

* Corresponding author.
E-mail address: somoza@gl.fcen.uba.ar (R. Somoza).

0012-821X/$ – see front matter © 2012 Elsevier B.V. All rights reserved.
doi:10.1016/j.epsl.2012.03.003

motions in western South America and some models of "absolute" plate motion have been routinely applied to give a plate tectonic context in many of the studies reporting new research in the Andes.

The available kinematic models on convergence in western South America vary depending on the quality and quantity of available information when each study was performed. The present contribution is an expansion of the study of Somoza and Ghidella (2005), who reported updated relative motions between South America and three of the oceanic plates subducted beneath the continent since Late Cretaceous: Phoenix, Farallon and Nazca. As in that contribution, the present one omits the analysis of the Antarctica–South America convergence because of the durability of the work of Cande and Leslie (1986). Basically, the Neogene history of convergence in western South America is as it was reported by Somoza (1998) for the Nazca–South America pair and by Cande and Leslie (1986) for the Antarctica–South America pair. Our results and interpretations for the Paleogene and Late Cretaceous times strongly differ from those in some of the previous investigations (e.g. Pardo Casas and Molnar, 1987; Pilger, 1984).

In that follows we show, first, a short comparative analysis of the models of Pilger (1984), Pardo Casas and Molnar (1987), Somoza (1998) and Somoza and Ghidella (2005). These studies were selected because their main subject is plate kinematics in the Andean margin and some of them are usually applied in tectonic investigations. Continuing, a new dataset of reconstructions is presented and some characteristics derived from these new data are discussed. Finally, it is shown that the South American motion as predicted by available hotspot (HS) models has insufficient resolution to analyze the Cenozoic evolution of the Andes.

2. Comparisons between some previous estimates of Nazca (Farallon) convergence kinematics in western South America

Several models describing the Cenozoic kinematics of convergence in western South America are available in the literature and some of them are routinely applied for tectonics interpretations. Although the models may basically agree with each other for the Late Cenozoic, they strongly differ in their Early Cenozoic predictions. This makes a comparison and a brief discussion on the origin of the between-model differences particularly pertinent.

All of these previous studies agree that the convergence direction was dominantly ENE–WSW in the Late Cenozoic and that it was roughly NE–SW in the middle to late Paleogene. The kinematic parameters for Late Cretaceous to Early Eocene times are different with no coherent pattern, leading both Pilger (1984) and Pardo Casas and Molnar (1987) to point out the difficulties in interpreting the kinematics of Farallon–South America during those times. Cande and Leslie (1986) first envisaged the possibility of subduction of the Phoenix plate in central and perhaps also in northern Chile during early Paleogene, a scenario that was reinforced by Somoza and Ghidella (2005) after applying recently available improvements in plate reconstructions (see below).

Fig. 1a–d shows the Middle Eocene to Recent convergence rate between Nazca (Farallon) and South America as predicted in four

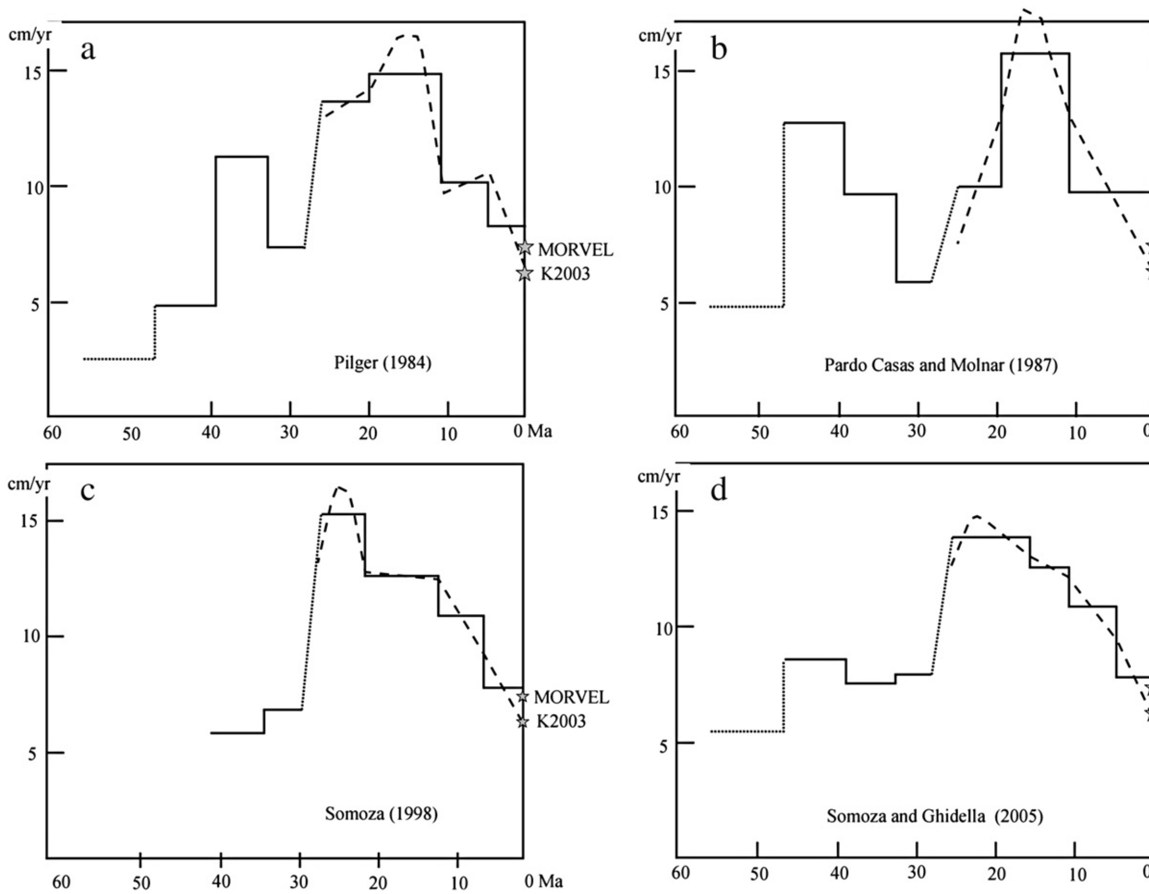

Fig. 1. Convergence rate at 22°S as predicted by a) Pilger (1984), b) Pardo Casas and Molnar (1987), c) Somoza (1998), d) Somoza and Ghidella (2005)*. Stars indicate the geologically current plate motion MORVEL model (DeMets et al., 2010) and instantaneous velocities from GPS (Kendrick et al., 2003). Solid lines represent average velocities for each of the discrete time intervals listed in Table 1. Dashed lines represent a simple, continuous variation of velocity that satisfy the present day GPS datum (Kendrick et al., 2003) and the average velocity within each interval (see main text).* Note that, because an error in the presentation, the convergence rate from the 11–16 Ma and 16–26 Ma intervals in Fig. 2 of Somoza and Ghidella (2005) is average together into a single 11–26 Ma interval. The individual values for the 11–16 Ma and 16–26 Ma intervals can be seen in their Cuadro (Table 1).

previous studies (Pardo Casas and Molnar, 1987; Pilger, 1984; Somoza, 1998 and Somoza and Ghidella, 2005). In all of the cases the age of magnetic chrons is assigned according to the Cande and Kent (1995) timescale. Somoza and Ghidella (2005) have shown that using the timescale of Gradstein et al. (2004) produces almost the same convergence rates for the 0–16 Ma interval, and small differences (~5%) for most of remainder intervals with exceptions of the 33–40 Ma (~15% faster) and 47–56 Ma (~15% slower) intervals.

Convergence rates vary along the margin as the distance between the observation point and the pole of rotation changes. For simplicity, the velocities in Fig. 1 correspond to an observation point close to the trench at 22°S, and the Late Cretaceous-Paleocene convergence rate is not shown because it will be discussed separately below. To analyze these diagrams it is worth remembering that they primarily represent a set of averaged velocities for discrete time intervals. Although we cannot know the evolution of velocities as a continuous curve, the area enclosed by the averaged velocity within each discrete time interval must be the same as the area enclosed by the unknown curve corresponding to the actual variation of velocity through time (i.e. area = space = $\int v\,dt$). The present day convergence rate determined by GPS measurements adds an additional constraint, so the dashed lines in the curves of Fig. 1 show an arbitrary continuous-variation of velocity that satisfies both the GPS datum and the averaged velocity within each interval as defined by sea-floor data, resulting that the areas below solid and shaded curves are the same. We do not claim that these shaded curves represent the actual continuous-variation of velocity through time but our intention is to illustrate the simpler curve that agrees with available constraints.

The curves in Fig. 1 show noticeable differences in Paleogene convergence rate. The Pardo Casas and Molnar's curve shows a strong maximum averaged-velocity in the 47–40 Ma interval, and a strong minimum in the 33–28 Ma interval; whereas the Pilger (1984) curve shows a strong maximum averaged-velocity between 40 and 33 Ma and a remarkable minimum between 47 and 40 Ma, exactly when the Pardo Casas and Molnar's curve predicts the maximum convergence rate. In contrast, Somoza and Ghidella (2005) show a rather constant convergence rate between Middle Eocene and Late Oligocene (Fig. 1), which is similar to the tendency shown by the short (going back to just 40 Ma) Oligo-Eocene curve in Somoza (1998). Somoza and Ghidella (2005) analyzed the source of the Late Cretaceous and Early Cenozoic differences between their model and the previous ones, and concluded that the main cause of differences arises from important improvements in reconstructions of South America–Africa (Cande et al., 1988; Shaw and Cande, 1990) and of Marie Byrd Land-Pacific (Cande et al., 1995). In contrast, they noted that application of different Africa–East Antarctica rotations (e.g. Molnar et al., 1988; Norton, 1995; Royer and Chang, 1991) does not significantly change the results.

The contrasts between the Neogene part of the models in Fig. 1 are smaller than in those for the late Paleogene part, with the observed discrepancies being related to the methodology that underlie each curve. The Neogene curves from Somoza (1998) and Somoza and Ghidella (2005) are mostly made using reconstructions between Nazca and adjacent oceanic plates derived from seafloor data (Tebbens and Cande, 1997). The ~25–16 Ma curve of Somoza and Ghidella (2005) is smoothed with respect to the coeval curve from Somoza (1998) because they omitted the convergence rate from his ~20–16 Ma (chrons 6o-5C) interval because its associated convergence direction was rather discordant with respect to the overall Neogene convergence direction, suggesting the possibility of some imprecision somewhere in the circuit (see discussion in Somoza, 1998). On the other hand, the curves from Pilger (1984), Somoza (1998) and Somoza and Ghidella (2005) show an overall decay of convergence rate during the Neogene, whereas this is not seen in the curve of Pardo Casas and Molnar (1987), which shows a maximum in the ~20–10 Ma interval in between two stages of lower velocities. These discrepancies are because available seafloor data in the 80's were not enough to define Nazca–Pacific or Nazca–Antarctica reconstructions younger than anomaly 7 times (~25 Ma). Thus, Pilger (1984) and Pardo Casas and Molnar (1987) estimated their younger Nazca–Pacific rotations by combining the anomaly 7 Nazca–Pacific reconstruction with present-day plate motion models available at that time (Chase, 1978; Minster and Jordan, 1978). Because in their conception, present-day plate motion models are assumed to be an acceptable representation of plate motions for the last 3 m.y. (Chase, 1978; DeMets et al., 1994, 2010; Minster and Jordan, 1978). Pilger (1984) assumed the validity of the Chase (1978) present-day plate motion for the last ~5 m.y., whereas Pardo Casas and Molnar (1987) extended the validity of the Minster and Jordan (1978) model for the last 10 m.y. These arbitrary (inescapable at the time) choices determine that the younger part of the plate kinematics model of Pilger (1984) is closer to the one dominated by seafloor data (Somoza, 1998) than the younger part of the Pardo Casas and Molnar (1987) model (Fig. 1).

3. Farallon (Nazca)–South America relative motions since Late Cretaceous

Relative motion between plates sharing a convergent boundary must be accomplished by adding finite rotations through a circuit of plates separated by mid-ocean ridges (e.g. Doubrovine and Tarduno, 2008a; Pardo Casas and Molnar, 1987; Pilger, 1984; Somoza, 1998). The plate circuit followed in this study is Nazca–East Antarctica–Africa–South America for the Middle Miocene (16 Ma) to Recent; and Farallon (Nazca)–Pacific–West Antarctica–East Antarctica–Africa–South America for the Late Cretaceous to Early Miocene (ca 20 Ma) reconstructions (see Supplementary data). Many individual rotations in the plate circuit derive from new seafloor data obtained from both mapping of seafloor using satellite radar altimetry data (e.g. Sandwell and Smith, 2009; and references therein) and new identifications of magnetic lineations, representing important improvements in plate reconstructions during the last 20 years (e.g. Cande et al., 1995, 2000, 2010; Croon et al., 2008; Müller et al., 1999; Norton, 1995; Royer and Chang, 1991; Shaw and Cande, 1990; Tebbens and Cande, 1997).

The magnetic chrons used in the reconstructions represent the same times as those from reconstructions involving the Nazca and/or Farallon plates. This way, the reconstructions from chron 3 to chron 5C correspond to the Nazca–Antarctica rotations of Tebbens and Cande (1997), whereas chron 7 and older reconstructions correspond to the set of Pacific–Farallon reconstructions of Pardo Casas and Molnar (1987) and Corrêa Rosa and Molnar (1988). Table 1 shows the new set of Nazca–Farallon to South America reconstructions for chrons 3o (4.9 Ma), 5o (10.8 Ma), 5Cy (16 Ma), 6o (20.2 Ma), 7y (24.8 Ma), 10y (28.3 Ma), 13 m (33.3 Ma); 18 m (39.6 Ma), 21 m (47 Ma), 25 m (56.1 Ma), 31y (67.7 Ma) and 32 m (71.2 Ma). The uncertainties in the rotations were determined according to the method described by Chang et al. (1990, see also Doubrovine et al., 2008b). In the Supplementary data we report the individual rotations in the plate circuit and the analytical values of mean convergence rate and mean convergence azimuth as seen at nine sites close to the Peru–Chile trench between 7°S and 49°S, plus an additional site at 3°N representing the Colombian–Ecuadorian Andes.

We divided the Late Cretaceous to Recent history of convergence between Farallon–Nazca and South America into three stages (Somoza and Ghidella, 2005). Fig. 2 shows the Euler poles that describe the clockwise rotation of the oceanic plate with respect to South America for each of the discrete time intervals enclosed by two successive finite rotations in Table 1. This figure illustrates the three-stage history of convergence, with the 25 to 0 Ma poles of Nazca plate forward motion (Fig. 2a) located close to western Wilkes Land, Antarctica, determining the roughly uniform ENE convergence of Nazca toward South America during Stage 1. The Nazca–South

Table 1
Finite reconstructions of Nazca (Farallon) to South America.

Chron	Age	Lat. (°N)	Long.	Angle	a	b	c	d	e	f
C3n.3n (o)	4.9	62.05	263.45	−3.87	0.327	0.287	−0.138	0.708	−0.226	0.488
C5n.2n (o)	10.8	63.93	262.81	−9.67	0.383	0.344	−0.031	0.953	−0.046	0.677
C5C.1n (y)	16.0	63.94	266.47	−15.04	0.982	0.770	−0.356	1.981	−0.840	1.263
C6n (o)	20.2	58.77	267.57	−20.12	2.667	−0.519	0.613	2.862	−0.128	0.760
C7n (y)	24.8	61.45	266.58	−26.05	3.074	−0.316	0.535	3.506	−0.542	1.227
C10n.1n (y)	28.3	66.54	258.65	−28.98	3.379	−0.439	0.927	3.784	−0.722	1.652
C13n (m)	33.3	68.25	243.93	−32.24	2.550	−0.492	1.047	2.982	0.112	0.743
C18n.2n (y)	39.6	68.82	226.57	−37.35	2.689	−0.465	1.068	3.377	−0.000	1.041
C21n (m)	47.1	68.32	214.01	−43.65	2.967	−0.372	1.085	4.162	−0.093	1.989
C25n (m)	56.1	68.50	183.87	−49.37	3.380	0.238	0.087	6.824	−0.240	6.467
C31n (y)	67.7	60.64	171.14	−54.96	8.856	3.391	−7.203	17.447	7.357	31.824
C32n.1n (m)	71.2	58.18	169.51	−55.75	17.255	7.683	−18.627	24.747	−0.092	51.398

Note: Chrons following nomenclature in Cande and Kent (1995), where o, m, y (old, middle, young, respectively) indicate the part of the subchron used to make the reconstruction.
Age is given in Ma.
The covariance matrix is given by the formula: $\begin{bmatrix} a & b & c \\ b & d & e \\ c & e & f \end{bmatrix} 10^{-5}$, where the values of a–f are given in radians.

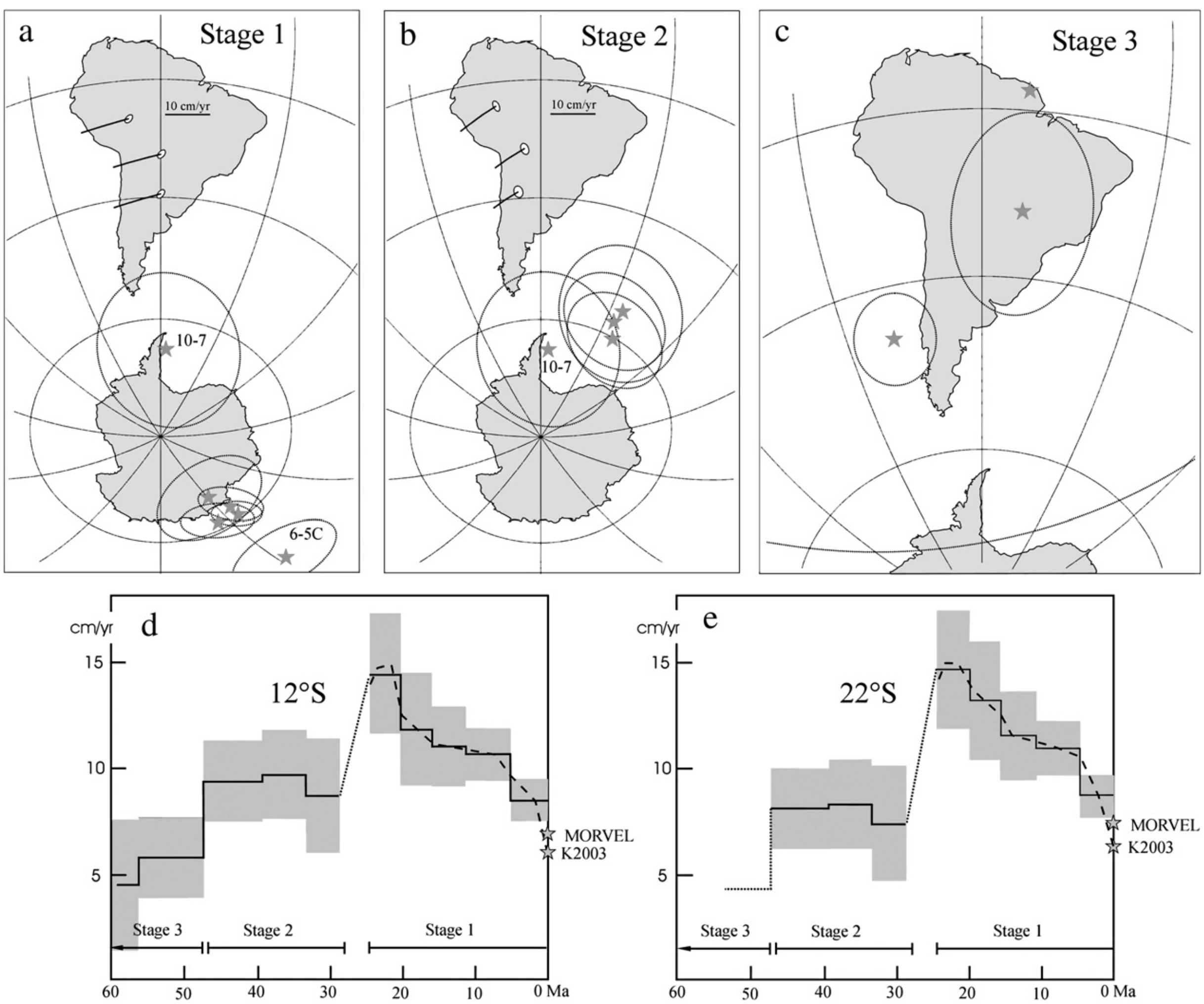

Fig. 2. Poles of rotation (clockwise) of Nazca (Farallon) to South America for each of the time intervals enclose by the reconstructions in Table 1, defining the three stage history of convergence since Late Cretaceous. a) the 25–0 Ma Stage 1, the overall ENE directed convergence of Nazca is illustrated by three velocity vectors close to the trench at 12°S, 22°S and 32°S. White ellipses show the map-view error of these convergence vectors. The pole representing the interval enclosed by anomalies 10–7 is interpreted as intermediate (see text for discussion). The pole representing the interval enclosed by anomalies 6–5C plot out of the cluster, see Supplementary data for discussion on the Nazca to Pacific anomaly 6 reconstruction. b) the 47–28 Ma Stage 2 characterized by NE convergence of Farallon along the margin. Examples of convergence vectors as in figure a. The pole for the interval enclosed by the anomalies 10 and 7 (see above) is also shown. c) the 72–47 Ma stage 3 characterized by northward migrating poles of rotation. Note that, for instance, the clockwise rotation of Farallon with respect to fixed South America associated to the 68–56 Ma pole does not predict convergence of the oceanic plate in central and southern Chile. The position of rotation poles of Stage 3 is somewhat sensitive to the reconstructions applied in the plate circuit, however the tendency for northward migration of stage poles and no subduction of Farallon in great part of the Chilean margin is observed irrespective of the used dataset (compare this figure with results in Somoza, 2005 and Somoza and Ghidella, 2005). d, e) convergence rate seen at 289°E, 22°S (d) and at 280°E, 12°S (e). Gray area shows the uncertainty in convergence rate. Dashed line in Stage 1 depicts the simpler curve that satisfies plate tectonic and GPS kinematic data for Stage 1.

America convergence rate for this stage begins with ~15 cm/yr average for the 25 to 20 Ma time interval followed by deceleration until reaching the present day instantaneous convergence velocity derived from GPS measurements (e.g. Fig. 2d,e) (see Supplementary data for similar results after applying an alternative plate circuit for the younger part of Stage 1).

For the 47 to 28 Ma interval (Stage 2; Fig. 2b) the poles are located close to the South Sandwich subduction zone, determining a NNE directed convergence in Patagonia becoming NE convergence farther north, imposing dextral obliquity in Chile, sinistral obliquity in southern Peru, and almost head-on convergence in central and northern Peru. The Farallon–South America convergence rate during Stage 2 is rather constant at the locality, varying along strike from ~6 cm/yr in northernmost Patagonia to ~10 cm/yr in northern Perú (Fig. 2d,e; see also Supplementary data). The latter contrasts with the results in some previous studies which show strong variations between Middle Eocene and Early Oligocene (Pardo Casas and Molnar, 1987; Pilger, 1984), highlighting the impact that the new improvements in the knowledge of seafloor fabric have on the plate circuit. Likewise, our estimates of convergence rate for the Cenozoic (see also Somoza and Ghidella, 2005) disagree with those presented by Sdrolias and Müller (2006), which show peaks at different ages and much higher Early Cenozoic values than ours. We suspect that at least part of these differences could be because Sdrolias and Müller (2006) used less accurate Farallon–Pacific rotations (see below) and because their dataset is not based on seafloor data only (such as ours) but incorporate HS kinematic models. It is worth mentioning that, in contrast with the wide agreement about the significance of seafloor fabric in the context of seafloor spreading theory, there is no consensus on the scope or even the validity of the deep mantle plume hypothesis (e.g. Anderson, 2000; Boschi et al., 2007, 2008; DePaolo and Manga, 2003; Foulguer and Natland, 2003; Sleep, 2006; see also www.mantleplumes.org), which by inference may affect the accuracy of its kinematic derivations. In agreement, we consider more confident and reliable the classical plate reconstructions based only on seafloor fracture zones and magnetic anomalies.

In contrast with the stability of poles of rotation in Stages 1 and 2, the Late Cretaceous to Early Eocene time span is characterized by important changes in the subduction zone. The poles of rotation for Farallon–South America tend to be close to the western continental margin without clustering in a particular zone (Fig. 2c), contrasting with that it is seen for the younger stages and suggesting a complex evolution of convergence for the Stage 3 (latest Cretaceous to Early Eocene). The mean pole of Farallon to South America rotation for the latest Paleocene to Early Eocene interval is located close to the western Patagonian margin, and the poles for older intervals are located farther north regardless of which set of reconstructions is applied in the plate circuit (Fig. 2c; see also Somoza, 2005; Somoza and Ghidella, 2005). Thus, it is likely that the poles in Fig. 3c do not represent stable convergence conditions within each of the three intervals between 56 and 71 Ma but they represent the average of variable kinematic conditions associated to a rather continuous shift of the instantaneous pole of convergence during pre-Middle Eocene times.

As noted above, the motion of the oceanic plate toward South America for each interval is represented by clockwise rotation about the stage poles shown in Fig. 2. In this context, and regardless the possible variability of convergence parameters, the 68 to 56 Ma stage pole indicates that the Farallon plate diverged from southern and possibly also central Chile (Fig. 2c) during the latest Cretaceous and most of the Paleocene. Evidences of subduction along the whole

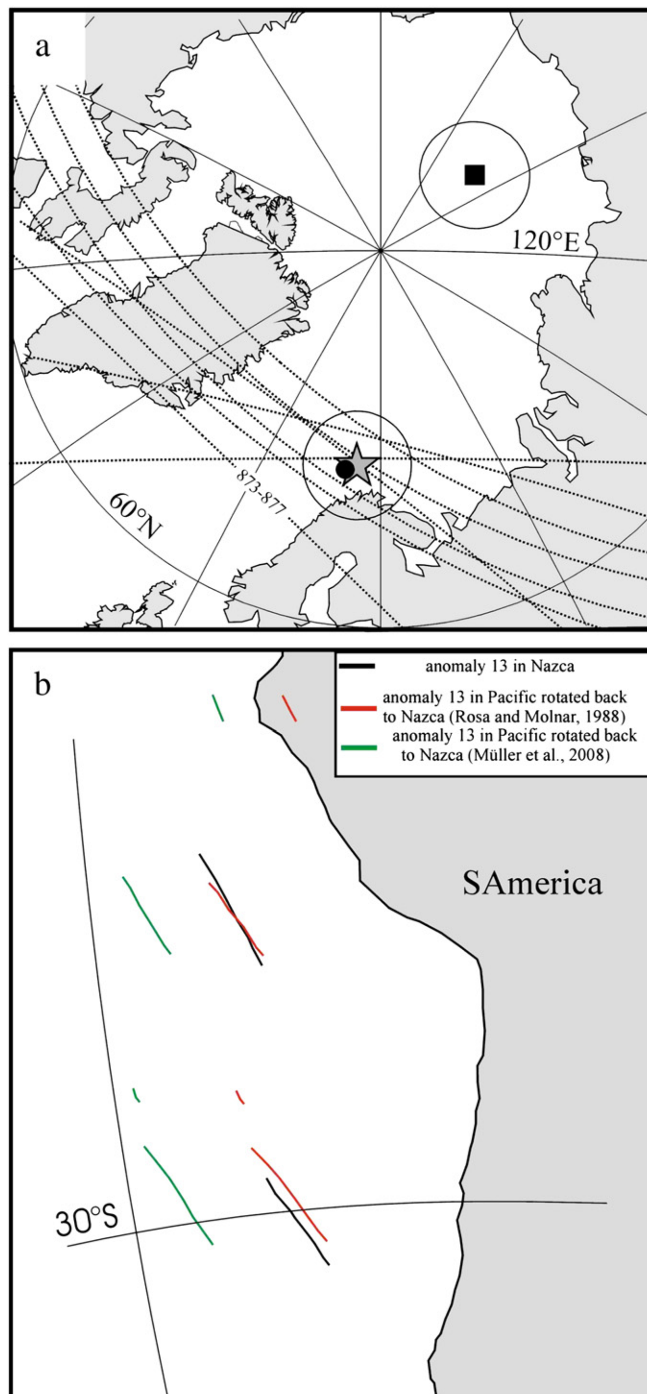

Fig. 3. a) Solid square represents the Late Cretaceous paleomagnetic pole for South America (Somoza and Zaffarana, 2008). Star in the same paleopole in Pacific coordinates using the plate circuit and reconstructions in this paper. Dot is the same paleopole applying the alternative plate circuit passing from East Antarctica to Australia, then to Lord Howe Rise and finally to the Campbell Plateau in the Pacific plate (Steinberger et al., 2004). Note that both plate circuits essentially conduct to the same result. Dashed curves are Late Cretaceous paleomagnetic colatitudes from DSDP and ODP basalt cores listed by Sager (2006). The paleomagnetic data from cores 163, 433c, 1203, 165a, 871, 883 and 884 are concordant with the reconstructed position of the Late Cretaceous pole of South America, whereas the colatitude from core 873–877 is the only discordant datum from the Pacific. This result supports the validity of both the plate circuits connecting the Indo-Atlantic and the Pacific realms.b) Black solid line represents the magnetic anomaly 13 in the Nazca plate. Red line represents its conjugate in the Pacific plate rotated back to Nazca using the reconstruction of Corrêa Rosa and Molnar (1988). Green line is the same Pacific magnetic anomaly rotated back to Nazca applying the reconstruction of Müller et al. (2008) (also Sdrolias and Müller, 2006). The result illustrates the different accuracy between the Pacific–Farallon reconstructions of Corrêa Rosa and Molnar (1988) and others available in the literature (see text for further discussion). (For interpretation of the references to color in this figure legend, the reader is referred to the web version of this article.)

Andean margin since the Jurassic and lack of Late Cretaceous-Paleocene marginal basins in Chile points that the simpler solution for the above observation is subduction of another plate, the likely candidate be the Phoenix plate, as it was first envisaged by Cande and Leslie (1986). This interpretation further predicts a southward migrating triple junction along great part (most?) of the Chilean margin from the latest Cretaceous to possibly Early Eocene times. Overall, the latest Cretaceous to earliest Cenozoic subduction of the Farallon plate beneath Chile was rather slow with variable direction in concert with the southward migration of the triple junction, at time that south of the triple junction the subduction of the Phoenix plate was rapid (> 10 cm/yr) and ESE–WNW directed (see below). This interpretation, based on observation of seafloor tectonic fabric, strongly contrasts with the scheme of Sdrolias and Müller (2006), who based on a hybrid model including HS and less accurate rotations (see below) mentioned subduction of the Pacific–Farallon and Pacific–Antarctic ridges beneath the Andes, which is negated by the seafloor fabric in the South Pacific (e.g. the traces of the Pacific–Phoenix–Farallon and Pacific–Antarctica–Farallon triple junctions, see Figs. 4, 5).

The transition from Stage 2 to Stage 1 is a major Cenozoic event in the plate kinematics of western South America, and is likely related to the process that led to the split of the Farallon plate to form the Nazca and Cocos plates (e.g. Lonsdale, 2005). Somoza and Ghidella (2005) discussed that the accuracy of the high convergence rates determined for the early Stage 1 depends on the reliability of the Early Miocene reconstructions between Pacific and Nazca. Direct (seafloor derived) determination of reconstructions for those times has been difficult because plate boundary reorganizations and microplate formations in the central Pacific basin produce gaps in the coverage of magnetic anomaly identifications. In fact, the Early Miocene Pacific–Nazca rotations in previous studies were based on interpolations involving reconstructions of anomaly 7 (~24.8 Ma; Pardo Casas and Molnar, 1987; Pilger, 1984) or anomaly 8 (~25.8 Ma; Somoza, 1998; Somoza and Ghidella, 2005). Recent studies (Barckhausen et al., 2008), however, attained reliable identifications of magnetic anomalies in the central Pacific and determined new Nazca to Pacific rotations for anomalies 6By (22.6 Ma) and 6Co (24.12 Ma). We used these data to obtain a new Nazca to South America reconstruction for anomaly 6By which allowed calculating a 22.6–16 Ma stage reconstruction. The associated 22.6–16 Ma Nazca–South America mean convergence rate at 22° S is ~16 cm/yr, compatible (slightly higher) with the velocities shown in Fig. 2d. The data, then, strongly suggest that the increase in convergence rate between Stage 2 and Stage 1 is not an artifact related to scarcity of magnetic anomaly identifications in the central Pacific but a real feature of the plate kinematics in western South America.

Another point to explore is how long the transition from Stage 2 to Stage 1 was. The major plate tectonic event in those times was the division of the Farallon plate into the Nazca and Cocos plates. In this context, the old boundary of our Stage 1 (anomaly 7, ~25 Ma) predates the earliest seafloor associated to the Nazca–Cocos ridge

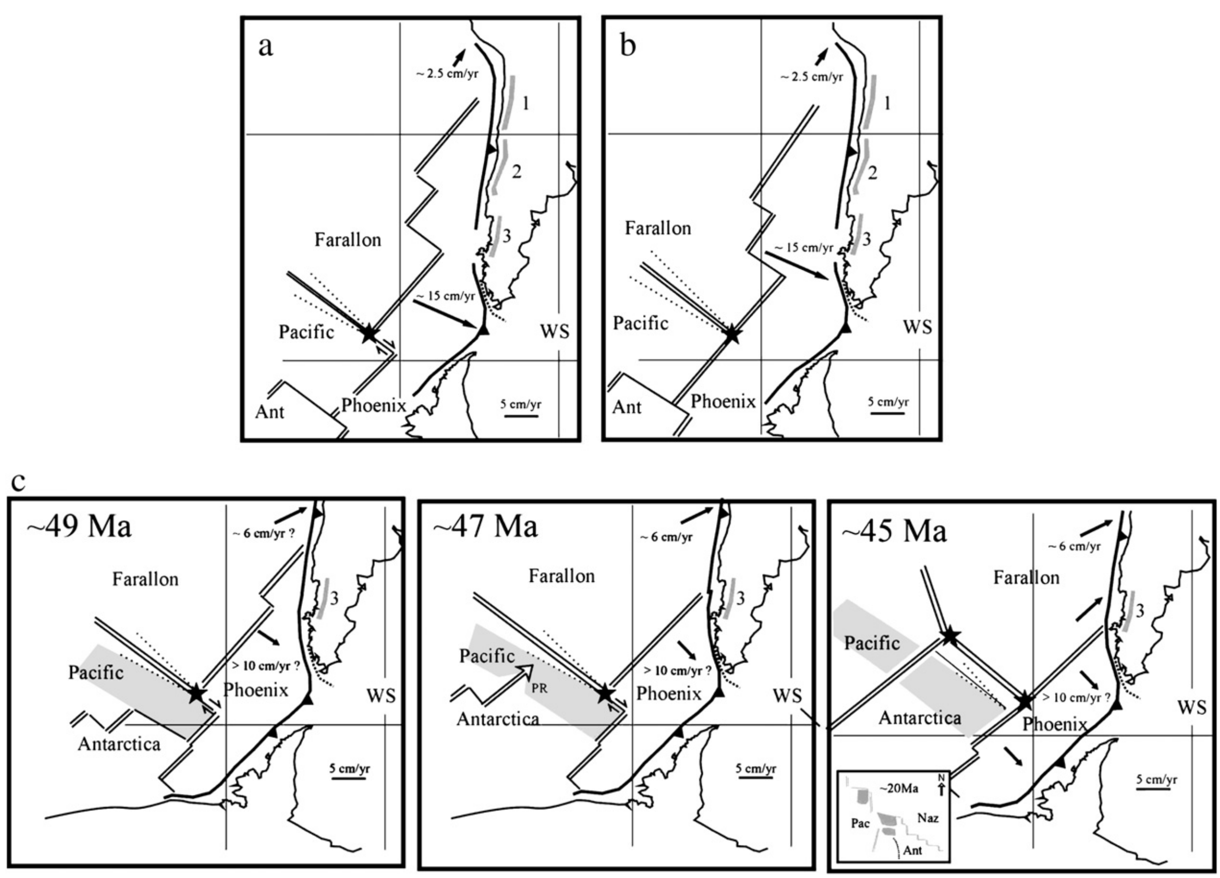

Fig. 4. a, b) Two possible configurations of the Pacific–Farallon–Phoenix triple junction (star) in the Late Cretaceous (72 Ma). The triple junction is positioned with respect to South America with the same rotation used in Fig. 3b. The inferred trend of the Farallon–Phoenix plate boundary is shown with an arbitrary geometry (arrangement of ridge and transform segments). The Phoenix to South America convergence direction is also shown. WS denotes Weddell Sea. Numbers in western South America indicate: (1) region with latest Cretaceous–earliest Paleocene deformation and intraplate like magmatism; (2) region with apparent absence of magmatism in the Paleocene; (3) region with Eocene deformation and slab-window volcanism (see further discussion in Somoza, 2005 and Somoza and Ghidella, 2005).c) One effect of the Eocene plate reorganization in the southeast Pacific (after Cande et al., 1982). Gray zone is seafloor created in the Phoenix–Pacific ridge. A propagating ridge (PR) allows a piece of this sea floor to be captured by the Antarctic plate (45 Ma map) where it is currently preserved. Inset in the 45 Ma map shows the configuration of the Pacific–Antarctica–Nazca triple junction at 20 Ma, with gray zones showing mid-ocean microplates (after Tebbens and Cande, 1997). Note that velocity vectors are not to scale but see values.

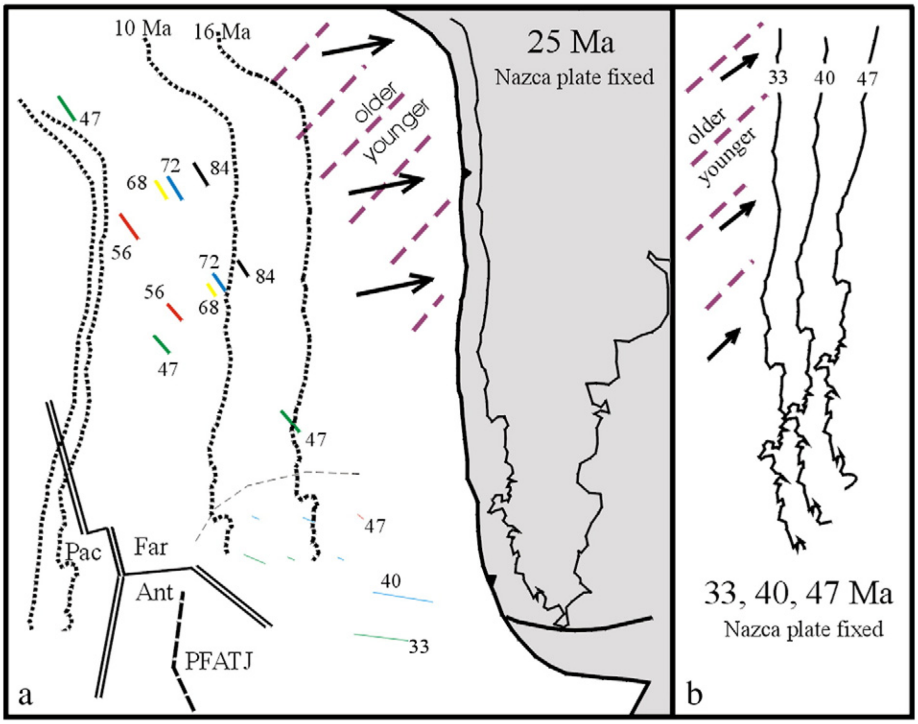

Fig. 5. a) Paleogene-Cretaceous magnetic lineations from the Pacific and Antarctica, and the Antarctica-Nazca-Pacific triple junction rotated back to Nazca plate. South America is shown at its 25 Ma (solid line), 16 and 10 Ma (both dotted lines) positions with respect to Nazca. The present-day position of South American coastline and the trench al also shown by dotted lines (0 Ma). Note that all illustrated oceanic floor has been subducted. Number identifies Pacific and Antarctic magnetic anomalies (each one denoted by a particular color). PFATJ is the trace of the Pacific-Farallon-Antarctica triple junction (Tebbens and Cande, 1997). Purple dashed lines represent the interpretation of magnetic lineaments in the Nazca (Farallon) plate with origin in the Farallon-Phoenix spreading center, with the age of sea floor increasing towards the northwest. Progressively older oceanic lithosphere originated at the Farallon-Phoenix ridge was subducted from ~24 to ~16 Ma, changing to subduction of progressively younger lithosphere belonging to the Farallon-Pacific ridge from ~16 Ma till present. Note that in northern Chile the change occurred at about 10 Ma, roughly coincident with the acceleration of uplift of the Central Andean plateau. b) South America reconstructed to Nazca for 33, 40 and 47 Ma (Stage 2 times). The reconstruction suggests that the inferred Farallon-Phoenix magnetic lineations (age increasing toward the northwest) were almost parallel to the convergence direction during Stage 2, suggesting that the age of subducted lithosphere at a certain site in the trench changed little when a single spreading corridor is subducted.

(~23 Ma; Barckhausen et al., 2008; Lonsdale, 2005). In fact, the anomaly 7 magnetic lineations in the central Pacific look parallel to the trend of the late Paleogene magnetic lineations, and the change to a new, Nazca-type trend begins to be observable from anomaly 6C (~24 Ma) lineations. The latter characteristics led Lonsdale (2005) to suggest that the entire Farallon plate began to rotate to a Nazca-like orientation just before its final rupture. This is likely why, although the 25–20 Ma rotation of the oceanic plate to South America includes pre- and post-breakup seafloor data, the corresponding pole is not intermediate between Stage 2 and Stage 1 but looks as part of the Stage 1 cluster (Fig. 2a). In contrast, the Farallon to South America pole for the ca 28–25 Ma interval (anomalies 10–7) plots in an intermediate position between the Stage 2 and Stage 1 clusters (Fig. 2a,b), and its associated mean convergence rate (~11 cm/yr at 22°S) is also intermediate between the late Paleogene and the latest Oligocene-earliest Miocene convergence rates shown in Fig. 2d. It is likely then, that the rotation of the 28–25 Ma interval averages variable convergence conditions related to the shift from Stage 2 to Stage 1. We conclude that the passage from Stage 2 to Stage 1 convergence types in western South America would have been gradual, preceding by some m.y. the creation of seafloor in the Cocos–Nazca spreading axis.

The transition from Stage 3 to Stage 2 in Peru is characterized by an increase in the Farallon–South America convergence rate (Fig. 2d). This acceleration of convergence coincides in time with the Paleogene increase discussed by Pardo Casas and Molnar (1987), although it is remarkably less abrupt. On the other hand, our paleogeographic interpretation points out that the equivalent increase in Chile would have been preceded by a slowdown associated to the passage of the triple junction at the site (i.e. Phoenix to South America convergence was substantially faster than Farallon to South America convergence during early Paleogene times, see above).

4. Discussing some aspects of the reconstructions and of the plate circuit

Although the West Indian Ridge System (WIRS) was the plate boundary between East Antarctica and Africa since the break-up of Gondwana, several reconstructions between these plates were made by combining data from the western, central and eastern Indian mid-ocean ridges (e.g. Molnar et al., 1988; Royer and Chang, 1991) which allowed a more complete and robust set of Africa–East Antarctica rotations. However, the development of the East Africa Rift System in the Late Cenozoic divided the eastern half of Africa into three independent plates (Nubia, Lwandle, and Somalia), whose roughly N–S boundaries merged in the WIRS, which passed thus to be the boundary of each of them with East Antarctica. In the last years they were improvements in the knowledge of the relative motion between these four plates sharing the WIRS in the late Neogene (e.g. DeMets et al., 2010; Homer-Johnson et al., 2007; Royer et al., 2006). Cande et al. (2010) have shown that the small amount of late Neogene relative motion between these four plates have little impact on the Early Cenozoic finite rotations between East Antarctica and Africa that are determined by considering Africa as a single plate all the time. Likewise, we found that correcting the Neogene rotations in order to obtain true East Antarctica to West Africa (Nubia) reconstructions produces small changes in the Nazca to South America convergence parameters obtained by assuming Africa as the single, pre-Great Rift Valley African-plate. In fact, the rotations with and without the corrections lead to similar Nazca to South America convergence direction, whereas the corrected dataset produces a small (< 0.5 cm/yr) increase in convergence rate for the younger intervals.

For many years, the possibility of an important although unaccounted amount of motion between West and East Antarctica has been invoked as one of the possible causes for disagreement between paleomagnetically determined paleolatitudes and those determined assuming motion of the Pacific plate with respect to a fixed HS grid (e.g. Acton and Gordon, 1994; Gordon and Cox, 1980). As an alternative to resolve this disagreement, it was proposed that there existed an unobserved plate boundary within the Pacific basin south of 45°S (Acton and Gordon, 1994; Corrêa Rosa and Molnar, 1988; Engebretson et al., 1984; Gordon and Cox, 1980; Gordon and Jurdy, 1986). Research in the last decade has shown that the Cenozoic relative motion between East and West Antarctica seems to be very small (e.g. Cande et al., 2000), suggesting that the disagreement between paleomagnetism and fixed Pacific HS models could be an intrinsic problem in the conception of the latter (e.g. Cande et al., 1995; Norton, 1995; Tarduno et al., 2003). Using the East to West Antarctica step in the plate circuit, we have shown (Somoza, 2005; Somoza and Ghidella, 2005) that the South American pole for the Late Cretaceous agrees very well with coeval paleomagnetic data from the Pacific, further supporting little motion between the Antarcticas since Late Cretaceous (see also Doubrovine and Tarduno, 2008b). This is illustrated in Fig. 3a after applying this plate circuit and the set of reconstructions used in this paper.

Nevertheless, an alternative plate circuit connecting Indo-Atlantic and Pacific realms has been recently proposed (Steinberger et al., 2004), which passes from East Antarctica to Australia, then to Lord Howe Rise and finally to the Campbell Plateau in the Pacific plate. Fig. 3a shows that the paleomagnetic test using this alternative plate circuit gives the same result as when the East–West Antarctica circuit is applied (see also Doubrovine and Tarduno, 2008b). Thus, Fig. 3a provides paleomagnetic support to both the occurrence of small relative motion between East and West Antarctica at least since 71 Ma (Cande et al., 2000) and the fit between Lord Howe Rise and Campbell Plateau proposed by Steinberger et al. (2004).

The fit between Late Cretaceous paleomagnetic data from the Pacific and South America indicates that any unobserved problem in determining the Farallon–South America kinematics would arise from inaccuracies in the Late Cretaceous to Early Cenozoic spreading history of the Pacific–Farallon ridge. The Pacific–Farallon reconstructions older than anomaly 13 (~33 Ma) are based on seafloor data from the Pacific plate alone and assuming symmetric spreading in the Pacific–Farallon ridge (e.g. Corrêa Rosa and Molnar, 1988). Somoza and Ghidella (2005) explored the possibility of persistent asymmetric spreading in the Pacific–Farallon ridge as the cause for the observed shift of the Late Cretaceous to Early Eocene stage poles in Fig. 2c. They applied up to 50% of accumulated asymmetric spreading for each of the ~10 m.y. time intervals that represent each of the stage rotations shown in Fig. 2c, a value that is larger than any observed seafloor spreading asymmetry since the Late Cretaceous (Müller et al., 1998). Somoza and Ghidella (2005) found that the assumed asymmetry does not change the northward shift tendency shown by the stage poles, strongly increasing it when the supposed asymmetry persistently favors the Pacific plate.

Recent reevaluation of Farallon–North America relative motions (Doubrovine and Tarduno, 2008a) used plate circuits based on both the Indo-Atlantic to Pacific paths mentioned above and two different sets of Pacific–Farallon reconstructions: Engebretson et al. (1984) and Müller et al. (2008). In contrast, we used the Late Cretaceous to Paleogene reconstructions of Corrêa Rosa and Molnar (1988) for the Pacific–Farallon pair (see also Somoza, 2005; Somoza and Ghidella, 2005). Cande and Haxby (1991) have shown that the Pacific–Farallon rotations of Corrêa Rosa and Molnar (1988) lead the Late Cretaceous and Paleogene magnetic anomalies in the Pacific to a better agreement with their conjugates preserved in the Nazca plate than the reconstructions of Mayes et al. (1990) do (see Fig. 8 in Cande and Haxby, 1991). Fig. 3b shows a comparison between the anomaly C13 reconstructions of Corrêa Rosa and Molnar (1988) and that of Müller et al. (2008) (also Sdrolias and Müller, 2006) after rotating the C13 magnetic chron in the Pacific back to the Nazca plate. The result clearly shows that the reconstruction of Corrêa Rosa and Molnar (1988) is acceptably accurate whereas the one from Müller et al. (2008) is not accurate, and the same age reconstruction from Engebretson et al. (1984) (not shown) produces even worse correlation than the one of Müller et al. (2008). Similar result may be observed when older anomalies are compared, with the reconstructions of Corrêa Rosa and Molnar (1988) always showing a tendency to produce a better fit than others, although tight fits are not observed in these cases. These observations strongly suggest that the Pacific to Farallon reconstructions of Corrêa Rosa and Molnar (1988) are more accurate than others available in the literature, so it would be interesting to reexamine the recently determined Farallon to North America relative motions and their tectonic implications (Doubrovine and Tarduno, 2008a) by using the Corrêa Rosa and Molnar (1988) Pacific–Farallon rotations.

5. Exploring the latest Cretaceous to Eocene Phoenix–South America convergence and speculations on the age of subducted lithosphere since Middle Eocene

The Cretaceous and Cenozoic plate tectonics in the southeast Pacific was dictated by interactions between the Pacific, Farallon, Phoenix and Antarctic plates. Information about the kinematics in the Pacific–Phoenix spreading center may be extracted from an almost continuous record of Cretaceous seafloor preserved west of the trace of the Pacific–Farallon–Phoenix triple junction in the Pacific plate (Cande et al., 1982; Larson et al., 2002) and from a piece of Paleocene-Early Eocene oceanic lithosphere that was originated in that ridge and later captured by the Antarctic plate (Cande et al., 1982). These records allow some estimation of Pacific–Phoenix relative motion assuming symmetric spreading. Somoza and Ghidella (2005) applied Antarctica–Phoenix rotations made by C. DeMets (in Gordon and Jurdy, 1986) to estimate the Phoenix–South America kinematics for latest Cretaceous-Paleocene times. They determined that the latest Cretaceous-Paleocene convergence between Phoenix and South America was ESE–WNW and rapid, about 14 cm/yr in southernmost South America. Overall, a fast (> 10 cm/yr) more or less ESE–WNW convergence of Phoenix in those times may be considered as a suitable working tool.

In contrast with the case of the Pacific–Phoenix spreading center, no seafloor formed in the Phoenix–Farallon ridge is preserved. However, some clues about the kinematics in the latter spreading center may be extracted by assaying closure of velocity triangles in the Pacific–Farallon–Phoenix triple junction (e.g. Larson et al., 2002), which suggests similar (~10–20° apart from each other) direction of spreading in both of the ridges that bounded the Phoenix plate nearby the triple junction (e.g. Larson et al., 2002; see also Fig. 4).

Reconstructing of the Phoenix–Farallon–Pacific triple junction with respect to South America and considering the above inference on the velocity triangles suggest that the latest Cretaceous-Paleocene magnetic lineations from the Phoenix–Farallon spreading center were oriented NE to NNE with respect to the present day continental margin, suggesting a NE to NNE oriented Phoenix–Farallon plate boundary, as Cande and Leslie (1986) first envisaged. It is worth mentioning that NE to NNE orientation for the Phoenix–Farallon plate boundary was also shown by the maps in Gordon and Jurdy (1986), although these authors reconcile the paleomagnetic and HS reference frames by including a distinct South Pacific plate (their Chatham Rise plate), the existence of which is not invoked in our analysis (Fig. 4, see also discussion in Section 4). Fig. 4a,b shows two possible paleogeographic scenarios for the southeast Pacific basin in the latest Cretaceous. Both of these options satisfy the requirements imposed by the position of the Pacific–Farallon–Phoenix triple junction with respect to South America, the preserved seafloor belonging from the Phoenix–Pacific spreading center in Antarctica (Cande et al., 1982) and the evidence against Farallon–South America convergence in most of Chilean margin shown in Fig. 2c. The true configuration of the Phoenix–Farallon plate boundary cannot be directly determined, nevertheless the Farallon–Phoenix–South America triple junction would have alternated between trench-ridge-trench (TRT) (likely dominant?) and trench–fault–trench (TFT) configurations.

The averaged southward motion of the triple junction would have been ≥20 cm/yr. Overall, lithosphere of the Phoenix plate subducted south of the triple junction converged much faster and was younger than Farallon lithosphere subducted north of triple junction. Along strike in the margin, the age of the subducted oceanic lithosphere increased faster north of the triple junction, where in turn progressive clockwise rotation of convergence direction during triple junction migration is predicted (see also Somoza and Ghidella, 2005). It is worth noting that our estimates of Phoenix–South America convergence are similar in both direction and rate to the estimates of convergence between Phoenix and West Antarctica during the Late Cretaceous-Paleocene (McCarron and Larter, 1998), in agreement with that would be expected by considering regional paleogeography.

The age of subducted oceanic lithosphere has been proposed as a possible factor in controlling the upper plate tectonics (e.g. Yañez and Cembrano, 2004). Closure of velocity triangles in the southward migrating Pacific–Farallon–Phoenix triple junction requires similar spreading direction for the Farallon–Phoenix and the Phoenix–Pacific ridges during mid-Cretaceous to Early Eocene times (Fig. 4; see also Larson et al., 2002). Fig. 5a shows Late Cretaceous and Paleogene magnetic anomalies of the Pacific plate from the Pacific–Farallon spreading center rotated back to the Nazca plate using the Corrêa Rosa and Molnar (1988) reconstructions. The figure also shows South America rotated back to its 25 Ma position relative to a fixed Nazca. The dashed lines represent the approximate trend of Farallon–Phoenix magnetic lineations in the Farallon plate, as predicted by paleogeography in Fig. 4. Considering the South America–Nazca convergence direction during Stage 1 (arrows), the figure proposes slight aging of subducted lithosphere at the site during Early Miocene passing to subduction of progressively younger lithosphere when this latter was the one originated in the Pacific–Farallon ridge. Fig. 5b shows the predicted situation for stage 2 times, when the Farallon–South America convergence direction was closer to the proposed trend of magnetic lineations from the Farallon–Phoenix ridge, suggesting that the age of oceanic lithosphere arriving at a certain position in the trench changed little from Middle Eocene to mid-Late Oligocene times. Thus, going from Fig. 5b to Fig. 5a allows a crude estimation of the age of subducted lithosphere since about Middle Eocene time. Note that this evolutionary model strongly contrast with the model of Sdrolias and Müller (2006), with which we must disagree (see discussion above, in Section 3).

6. On the “absolute” motion of the continental plate and Cenozoic Andean tectonics

Determining the motion of plates relative to the deep mantle would greatly improve our knowing of the plate driving forces and their relative contributions to plate tectonics. For more than three decades efforts were made to develop and refine absolute plate motion models based on HS tracks. This kinematic approach assumes that intraplate volcanic chains form because plates move over plumes that rise vertically from the lowermost mantle and have negligible motion in a mantle reference frame (e.g. Engebretson et al., 1984; Morgan, 1971; Müller et al., 1993; Wessel and Kroenke, 2008; Wilson, 1963). However, during the last years several workers have noted inconsistencies between paleomagnetic and fixed HS reference frames (Norton, 1995; Somoza and Zaffarana, 2008; Tarduno and Cottrell, 1997; Tarduno et al., 2003). The development of moving HS reference frames (O'Neill et al., 2005; Steinberger and O'Connell, 1998; Steinerger, 2000; Torsvik et al., 2008), based on mantle convection models and calibrated by paleomagnetic paleolatitudes, reduced

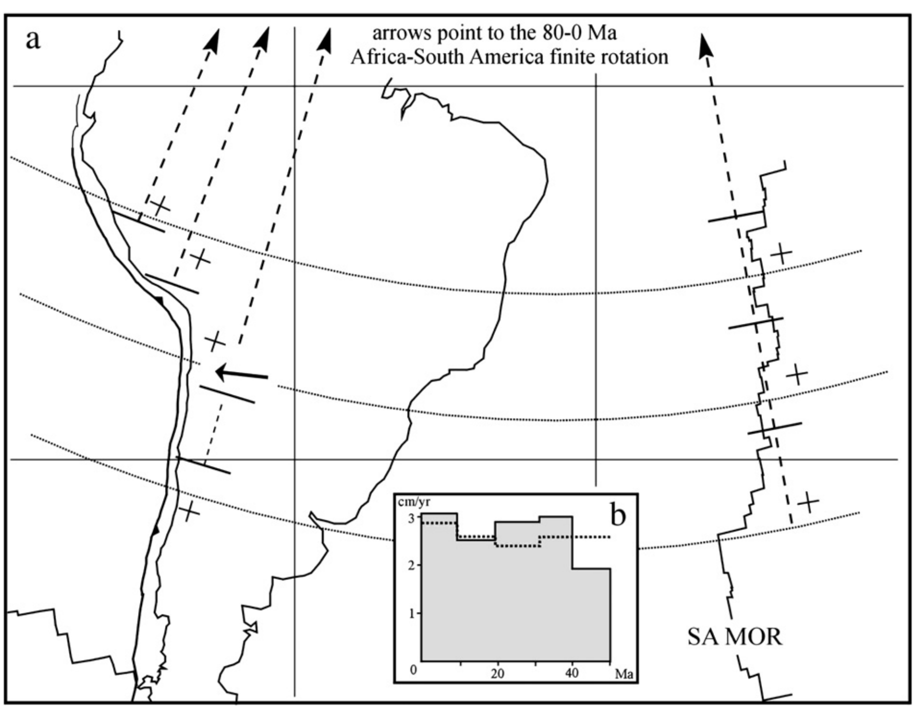

Fig. 6. Elements in the kinematic model of Silver et al. (1998). Arrows converge in the pole of 80 Ma finite reconstruction of South America and Africa (Shaw and Cande, 1990). Circles are small circles with respect to that reconstruction pole. Note that the South Atlantic mid-ocean ridge (SA MOR) is almost parallel to a meridian of the 80 Ma Africa to South America reconstruction pole. Gray area in the inset shows the South American motion with respect to the hot spot model of O'Connor and le Roex (1992), the one applied by Silver et al. (1998). Dotted line in the inset shows the full vector in Fig. 1 of Silver et al. (1998). See main text for discussion.

but not canceled the discrepancies between HS and paleomagnetic reference frames (Poblete et al., 2011; Somoza and Zaffarana, 2008).

In the last few years, some valuable contributions on Andean geodynamics (e.g. Babeyko and Sobolev, 2008; Oncken et al., 2006; Quinteros et al., 2006; Sobolev and Babeyko, 2005) were made by applying an "absolute" plate motion model arising from an approach that decomposes the South American motion with respect to the African hotspots into two rather arbitrary directions (Silver et al., 1998). Somoza and Ghidella (2005) criticized the methodology and the results of Silver et al. (1998) arguing that HS models lack the appropriate resolution to define changes in "absolute" upper plate motion suitable for their correlation with the Cenozoic evolution of the Andes.

Fig. 6 shows the main elements in Fig. 1 of Silver et al. (1998), where they show a decomposition of both the Africa–South America relative motion (Shaw and Cande, 1990) and the forward motion of Africa and South America with respect to the African hotspots (O'Connor and le Roex, 1992) into components parallel and perpendicular to the circles centered in the of 80 Ma finite reconstruction pole between Africa and South America (see Fig. 6). The South Atlantic mid-ocean ridge-system, oriented N10W (i.e. "approximately" N–S, as claimed by Silver et al., 1998), is almost parallel to a meridian of this finite reconstruction pole (Fig. 6). Thus, Fig. 1 in Silver et al. (1998) shows the velocity vectors decomposed into components approximately parallel and perpendicular to the South Atlantic mid-ocean ridge. Silver et al. (1998) show a Neogene increase in the component of velocity perpendicular to the mid-ocean ridge while at the same time their approach leads to a simultaneous decrease in the component of velocity parallel to the mid-ocean ridge. Somoza and Ghidella (2005) have shown that the vectorial sum of the Silver et al. (1998, their Fig. 1) components (i.e. their true velocity vectors) is almost constant for the last 50 m.y. (see inset in Fig. 6). In the Andean zone, the directions of the components perpendicular and parallel to the small circles centered in the 80 Ma South Atlantic finite rotation are about 20° arc removed from the E–W and N–S directions suggested by Silver et al. (1998) for their components (see Fig. 6). More important, these directions represent nothing related to Andean tectonics, because the true reference frame there should be imposed by the vector of "absolute" motion as seen in the Andean undeformed foreland and the trend of the boundary of the deformation zone (e.g. the continental margin), as it is considered in transpression analyzes. The approach of Silver et al. (1998) seems to be designed to analyze the behavior of transforms in the Africa–South America plate boundary instead of Andean tectonics.

Fig. 7 shows the results of South American motion with respect to HS applying the traditional methodology on several Indo-Atlantic (Fig. 7a) and Pacific (Fig. 7b) HS models. Overall, the results in Fig. 7 suggest that the temporal variations of South American "absolute" velocity as predicted by both fixed and moving HS models do not have enough resolution to be used for studying the Central Andean evolution in the Cenozoic.

Nevertheless, some qualitative aspects may be considered. Several lines of evidence suggest that the South Atlantic mid-ocean ridge was migrating westward since Late Cretaceous and this migration accelerated at times of the development and culmination of Africa–Europe collision (O'Connor and Duncan, 1990; Silver et al., 1998; Somoza and Zaffarana, 2008). This is because the combination of both the continued accretion of oceanic lithosphere in the South Atlantic ridge and the Africa slowdown since Late Cretaceous implies that the South Atlantic mid-ocean ridge episodically moved westward, with most of the expansion being accommodated by westward motion of South America. Both GPS derived data and estimates of present-day plate motion (DeMets et al., 2010; Jin and Wang, 2008) indicate about 3 cm/yr full spreading in the South Atlantic, whereas seafloor data indicate an average of 4 cm/yr for both the 0–9 Ma and the 9–19 Ma time intervals (e.g. Shaw and Cande, 1990). Thus,

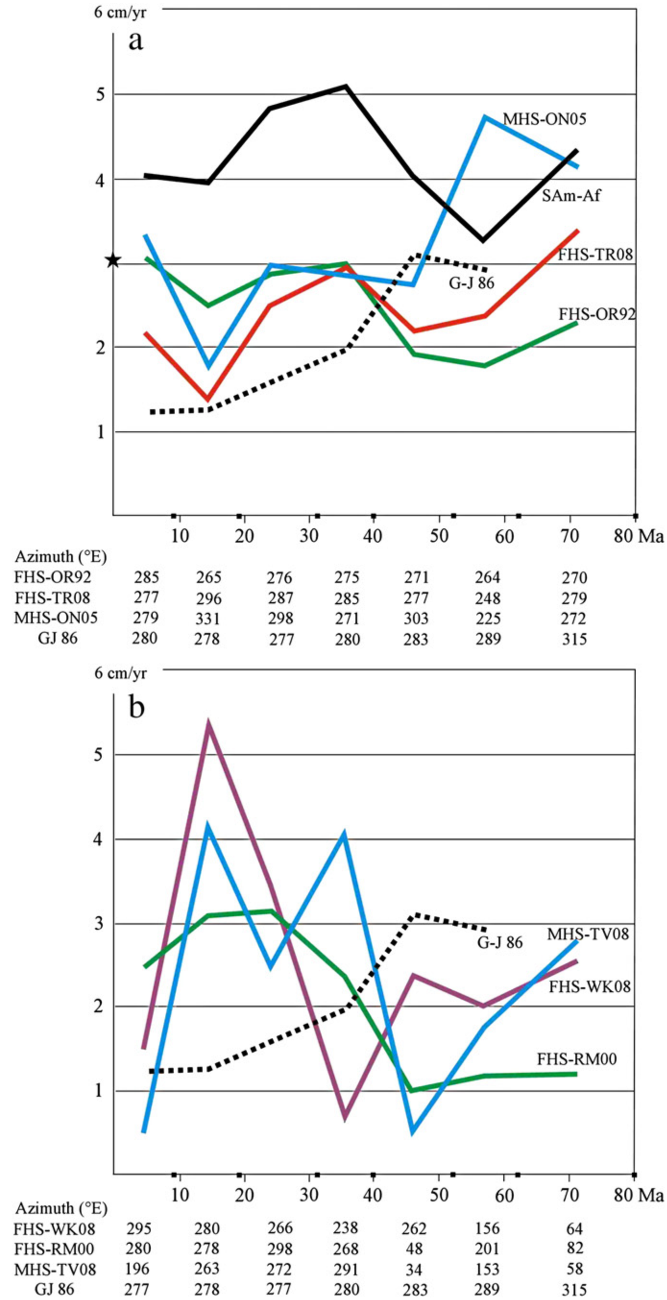

Fig. 7. Motion of South America according to hotspot models as seen in a foreland locality at 300°E, 20°S. Reconstructions are made for the same times used by Silver et al. (1998) and velocities are represented in the graph as they did in theirs. a) Indo Atlantic models: fixed hotspot models of O'Connor and le Roex (1992) and Torsvik et al. (2008) (FHS OR92 and FHS TV08, respectively), and moving hotspot model of O'Neill et al. (2005) (MHS ON05). Sam-Af represents the rate of full spreading in the South Atlantic according to reconstructions of Shaw and Cande (1990). Star is the rate of present-day Africa–South America relative motion derived from GPS measurements. The GJ86 curve represents the kinematics according to the mixed (Pacific and Indo-Atlantic) hot spot model of Gordon and Jurdy (1986). b) Pacific models: fixed hotspot models of Raymond et al. (2000) and Wessel and Kroenke (2008) (FHS RM00 and FHS WK08, respectively), and moving hotspot model of Torsvik et al. (2008) (MHS TV08). The mixed GJ86 curve is also shown together with the Pacific models.

kinematics in the South Atlantic (Fig. 7a) suggests an acceleration of full-spreading from about 3 to 5 cm/yr starting between 50 and 40 Ma and culminating at 30–35 Ma, followed by a deceleration from about 5 to 3 cm/yr in the last 20 m.y. In this context, and considering progressive African slowdown, it may be reasonable to consider that the South American "absolute motion" may have been between ~3 and ~4 cm/yr during the last 40 m.y., although it is not possible to quantitatively yield a reliable determination of the evolution of the velocity of continental drift.

7. Conclusions

The latest Cretaceous–Cenozoic convergence history in western South America may be divided into three stages. The youngest Stage 1 (25–0 Ma) is characterized by ENE directed convergence of the Nazca plate toward most of South America, and by ~E–W subduction of the Antarctic plate beneath southern Patagonia. In this stage, the convergence rate shows a continuous decrease from the highest value in the Cenozoic (average between 25 and 20 Ma) to the present day values measured by GPS. Stage 2 (47–28 Ma) is characterized by NE directed subduction of Farallon, with the convergence rate remaining almost constant during the entire interval. During those times obliquity was dextral in Chile, sinistral in southern Peru and almost head-on convergence occurred in central and northern Peru.

During latest Cretaceous to Early Eocene times (Stage 3) the Farallon plate was subducted beneath Perú and the Phoenix plate was subducted farther south, where a triple junction migrated southward along the Chilean margin. The subduction of Farallon was rather slow with variable direction imposed by the position of the triple junction, whereas subduction of Phoenix plate was rapid (>10 cm/yr) and ESE directed.

Comparison of Late Cretaceous paleomagnetic data from South America and Pacific confirms that the previously observed disagreement between paleomagnetically determined paleolatitudes in the Indo-Atlantic and Pacific realms and those determined assuming motion of Pacific plate with respect to a fixed HS grid is related to intrinsic problems of the fixed hotspot hypothesis. On the other hand, we present an exercise suggesting no major changes in the age of subducted lithosphere in the Chile trench from ~47 to ~28 Ma, followed by subduction of progressively older oceanic lithosphere from ~24 to ~16 Ma and finally changing to subduction of progressively younger lithosphere from ~16 Ma till present. Finally, it is shown that South American motion as predicted by available hotspot models has insufficient resolution to be applied to the analysis of Cenozoic Andean deformation.

Acknowledgments

Several figures were made using the GMAP32 program written by T. Torsvik and M. Smethurst. The reconstructions in this contribution are a reworked version of an early set of reconstructions prepared to be presented in the SFB 267 Andean Workshop at the Freie Universität Berlin, November 2003. R.S. thanks to the organizers, in special to Nina Kukowski, for the invitation to participate in that workshop. The exercise of estimating the age of subducted oceanic lithosphere was impelled by a question of Peter Giese. Review by Steve Cande improved an early version of the manuscript.

Appendix A. Supplementary data

Supplementary data to this article can be found online at doi:10.1016/j.epsl.2012.03.003.

References

Acton, G., Gordon, R.G., 1994. Paleomagnetic tests of the pacific plate reconstructions and implications for motion between hotspots. Science 263, 1246–1254.
Aleman, A., Ramos, V.A., 2000. Northern Andes. In: Cordani, U., et al. (Ed.), Tectonic Evolution of South America. 31st Int. Geol. Cong., Rio de Janeiro, Brazil, pp. 453–480.
Anderson, D.L., 2000. The thermal state of the upper mantle: no role for mantle plumes. Geophys. Res. Lett. 27, 3623–3626.
Babeyko, A.Y., Sobolev, S.V., 2008. High resolution numerical modeling of stress distribution in visco-elastic–plastic subducting slabs. Lithos 103, 205–216.
Barckhausen, U., Ranero, C.R., Cande, S.C., Engels, M., Weinrebe, W., 2008. Birth of an intraoceanic spreading center. Geology 36, 767–770.
Boschi, L., Becker, T.W., Steinberger, B., 2007. Mantle plumes: dynamic models and seismic images. Geochem. Geophys. Geosyst. 6 (4), Q100006. doi:10.1029/2007GC001733.
Boschi, L., Becker, T.W., Steinberger, B., 2008. On the statistical significance of correlations between synthetic mantle plumes and tomographic models. Phys. Earth Planet. Inter. 167, 230–238.
Cande, S., Haxby, W., 1991. Eocene propagating rifts in the southwest Pacific and their conjugate features in the Nazca plate. J. Geophys. Res. 96, 19609–19622.
Cande, S., Kent, D., 1995. Revised calibration of the geomagnetic timescale for the Late Cretaceous and Cenozoic. J. Geophys. Res. 100, 6093–6095.
Cande, S., Leslie, R., 1986. Late Cenozoic tectonics of the southern Chile trench. J. Geophys. Res. 91, 471–496.
Cande, S., Herron, E., Hall, B., 1982. The early Cenozoic tectonic history of the southeast Pacific. Earth Planet. Sci. Lett. 57, 63–74.
Cande, S., LaBrecque, J., Haxby, W., 1988. Plate kinematics of the South Atlantic: chron C34 to present. J. Geophys. Res. 93, 13479–13492.
Cande, S.C., Raymond, C., Stock, J., Haxby, W., 1995. Geophysics of the pitman fracture zone and Pacific–Antarctica plate motions during the Cenozoic. Science 270, 947–953.
Cande, S.C., Stock, J.M., Dietmar Müller, R., Ishihara, T., 2000. Cenozoic motion between East and West Antarctica. Nature 404, 145–150.
Cande, S.C., Patriat, P., Dyment, J., 2010. Motion between the Indian, Antarctic and African plates in the Early Cenozoic. Geophys. J. Int. 183, 127–149.
Chang, T., Stock, J., Molnar, P., 1990. The rotation group in plate tectonics and the representation of uncertainties of plate reconstructions. Geophys. J. Int. 102, 649–661.
Chase, C.G., 1978. Plate kinematics: the Americas, East Africa, and the rest of the world. Earth Planet. Sci. Lett. 37, 355–368.
Corrêa Rosa, J.W., Molnar, P., 1988. Uncertainties in reconstructions of the Pacific, Farallon, Vancouver, and Kula plates and constraints on the rigidity of the Pacific and Farallon (Vancouver) plates between 72 and 35 Ma. J. Geophys. Res. 93, 2997–3008.
Croon, M.B., Cande, S.C., Stock, J.M., 2008. Revised Pacific–Antarctic plate motions and geophysics of the Menard fracture zone. Geochem. Geophys. Geosyst. 9. doi:10.1029/2008GC002019.
Dalziel, I.W.D., 1981. Back-arc extension in the southern Andes: a review and critical reappraisal. Phil. Trans. R. Soc. Lond. A 300, 319–335.
DeMets, C., Gordon, R.G., Argus, A., Stein, S., 1994. Effect of recent revisions to the geomagnetic reversal timescale on estimates of current plate motions. Geophys. Res. Lett. 21, 2191–2194.
DeMets, C., Gordon, R.G., Argus, D.F., 2010. Geologically current plate motions. Geophys. J. Int. 181, 1–80.
DePaolo, D.J., Manga, M., 2003. Deep origin of hotspots—the mantle plume model. Science 300, 920–921.
Dewey, J., Bird, J., 1970. Mountain belts and the new global tectonics. J. Geophys. Res. 75, 2625–2647.
Doubrovine, P.V., Tarduno, J.A., 2008a. A revised kinematic model for the relative motion between Pacific oceanic plates and North America since the Late Cretaceous. J. Geophys. Res. 113, B12101. doi:10.1029/2008JB005585.
Doubrovine, P.V., Tarduno, J.A., 2008b. Linking the Late Cretaceous to Paleogene Pacific plate and the Atlantic bordering continents using plate circuits and paleomagnetic data. J. Geophys. Res. 113, B07104. doi:10.1029/2008JB005584.
Engebretson, D.C., Cox, A., Gordon, R.G., 1984. Relative motions between oceanic plates in the Pacific basin. J. Geophys. Res. 89, 10291–10310.
Feininger, T., Bristow, C.R., 1980. Cretaceous and Paleogene geologic history of coastal Ecuador. Geol. Rundsch. 69, 849–874.
Foulguer, G.R., Natland, J.H., 2003. Is "hotspot" volcanism a consequence of plate tectonics? Science 300, 921–922.
Ghiglione, M.C., Quinteros, J., Yagupsky, D., Bonillo-Martinez, P., Hlebszevrich, J., Ramos, V.A., Vergani, G., Figueroa, D., Quesada, S., Zapata, T., 2010. Structure and tectonic history of the foreland of southernmost South America. J. South Am. Earth Sci. 29, 262–277.
Gordon, R.G., Cox, A., 1980. Paleomagnetic test of the Early Tertiary plate circuit between the Pacific basin plates and the Indian plate. J. Geophys. Res. 85, 6534–6546.
Gordon, R.G., Jurdy, D.M., 1986. Cenozoic global plate motions. J. Geophys. Res. 91, 12389–12406.
Gradstein, F.M., et al., 2004. A Geologic Time Scale 2004. Cambridge University Press, Cambridge. 500 pp.
Hampel, A., 2002. The migration history of the Nazca ridge along the Peruvian active margin; a re-evaluation. Earth Planet. Sci. Lett. 203, 665–679.
Hartley, A.J., 2003. Andean uplift and climate change. J. Geol. Soc. 160, 7–10.
Homer-Johnson, B.C., Gordon, R.G., Argus, D.F., 2007. Plate kinematic evidence for the existence of a distinct plate between the Nubian and Somalian plates along the Southwest Indian Ridge. J. Geophys. Res. 112, B05418. doi:10.1029/2006JB004519.
Iaffaldano, G., Bunge, H.P., Dixon, T.H., 2006. Feedback between mountain belt growth and plate convergence. Geology 34, 893–896.
Jin, S., Wang, J., 2008. Spreading change of Africa–South America plate: insights from space geodetic observations. Int. J. Earth Sci. 97, 1293–1300.
Kendrick, E., Bevis, M., Smalley, R., Brooks, B., Bariiga Vargas, R., Lauría, E., Fortes, L.P., 2003. The Nazca–South America Euler vector and its rate of change. J. South Am. Earth Sci. 16, 125–131.
Lamb, S., Davis, P., 2003. Cenozoic climate change as a possible cause for the rise of the Andes. Nature 425, 792–797.
Larson, R.L., Pockainy, R.A., Viso, R.F., Erba, E., Abrams, L.J., Luyendyk, B.F., Stock, J.M., Clayton, R.W., 2002. Mid-Cretaceous tectonic evolution of the Tongareva triple junction in the southwestern Pacific basin. Geology 30, 67–70.
Liu, M., Yang, X., Stein, S., Klosko, E., 2003. Crustal shortening and extensión in the Central Andes: insights from viscoelastic model. In: Stein, S., Freymuller, G. (Eds.), Plate Boundary Zones: AGU Geodyn. Ser, 30, pp. 325–339.

Lonsdale, P., 2005. Creation of the Cocos and Nazca plates by fission of the Farallon plate. Tectonophysics 404, 237–264.
Martinod, J., Husson, L., Roperch, P., Guillaume, B., Espurt, N., 2010. Horizontal subduction, convergence velocity and the building of the Andes. Earth Planet. Sci. Lett. 299, 299–309.
Mayes, C.L., Lawver, L.A., Sandwell, D.T., 1990. Tectonic history and new isochron chart of the South Pacific. J. Geophys. Res. 95, 8543–8567.
McCarron, J.J., Larter, R.D., 1998. Late Cretaceous to early Tertiary subduction history of the Antarctica Peninsula. J. Geol. Soc. 155, 255–268.
McQuarrie, N., 2002. Initial plate geometry, shortening variations, and evolution of the Bolivian orocline. Geology 30, 867–870.
Mégard, F., 1987. Cordilleran Andes and marginal Andes: a review of Andean geology north of the Arica elbow (18°S). In: Monger, Francheteau (Eds.), Circum-Pacific belts and evolution of the Pacific Ocean basin: AGU, Geodyn. Ser., 18, pp. 71–95.
Minster, J.B., Jordan, T.H., 1978. Present-day plate motions. J. Geophys. Res. 83, 5331–5354.
Molnar, P., Pardo Casas, F., Stock, J., 1988. Uncertainties in the reconstruction of the Indian, African, and Antarctic plates since Late Cretaceous time. Basin Res. 1, 23–40.
Morgan, W.J., 1971. Deep mantle convection plumes and plate tectonics. AAPG Bull. 56 (2), 203–213.
Mpodozis, C., Ramos, V.A., 1990. The Andes of Chile and Argentina. In: Eriksen, G., et al. (Ed.), Geology of the Andes and Its Relation to Hydrocarbon and Mineral Resources, Circum-Pacific Council for Energy and Mineral Resources: Earth Sci. Ser., 11, pp. 59–90. Houston.
Müller, R.D., Royer, J.-Y., Lawver, L.A., 1993. Revised plate motions relative to the hotspots from combined Atlantic and Indian Ocean hotspot tracks. Geology 21, 275–278.
Müller, R.D., Roest, W.R., Royer, J.Y., 1998. Asymmetric sea-floor spreading caused by ridge–plume interactions. Nature 396, 455–459.
Müller, R.D., Cande, S.C., Royer, J.-Y., Roest, W.R., Machenkov, S., 1999. New constraints on the Late Cretaceous/Tertiary plate tectonic evolution of the Caribbean. In: Mann, P. (Ed.), Sedimentary Basins of the World. : Caribbean Basin, 4. Elsevier, New York, pp. 39–55.
Müller, J.P., Kley, J., Jacobshagen, V., 2002. Structure and Cenozoic kinematics of the Eastern Cordillera, southern Bolivia (21°S). Tectonics 21 (5), 1037. doi:10.1029/2001TC001340.
Müller, R.D., Sdrolias, M., Gaina, C., Roest, W.R., 2008. Age, spreading rates, and spreading asymmetry of the world's ocean crust. Geochem. Geophys. Geosyst. 9, Q04406. doi:10.1029/2007GC001743.
Norton, I., 1995. Plate motions in the North Pacific: the 43 Ma nonevent. Tectonics 14, 1080–1094.
O'Connor, J.M., Duncan, R.A., 1990. Evolution of the Walvis Ridge–Rio Grande Rise hot spot system: implications for African and South American plate motions over plumes. J. Geophys. Res. 95, 17475–17502.
O'Connor, J.M., le Roex, A.P., 1992. South Atlantic hot spot–plume systems: distribution of volcanism in time and space. Earth Planet. Sci. Lett. 113, 343–364.
O'Neill, C., Müller, R.D., Steinberger, B., 2005. On the uncertainties in hot spot reconstructions and the significance of moving hot spot reference frames. Geochem. Geophys. Geosyst. 6 (4), Q04003. doi:10.1029/2004GC000784.
Oncken, O., Hindle, D., Kley, J., Elger, K., Victor, P., Schemmann, K., 2006. Deformation of the Central Andean upper plate system—facts, fiction, and constraints for plateau models. In: Oncken, O., Chong, G., Franz, G., Giese, P., Götze, H.J., Ramos, V.A., Strecker, M., Wigger, P. (Eds.), The Andes. Active subduction orogeny. : Front. Earth Sci., 1. Springer, Berlin, pp. 3–27.
Pardo Casas, F., Molnar, P., 1987. Relative motion of the Nazca (Farallon) and South American plates since Late Cretaceous. Tectonics 6, 233–248.
Pilger, R.H., 1984. Cenozoic plate kinematics, subduction and magmatism: South American Andes. J. Geol. Soc. 141, 793–802.
Poblete, F., Arriagada, C., Roperch, P., Astudillo, N., Hervé, F., Kraus, S., le Roux, J.P., 2011. Paleomagnetism and tectonics of the South Shetland Islands and the Antarctica Peninsula. Earth Planet. Sci. Lett. 302, 299–313.
Quinteros, J., Jacovkis, P.M., Ramos, V.A., 2006. Evolution of the upper crustal deformation in subduction zones. J. Appl. Mech. Trans. ASME 73, 984–994.
Ramos, V.A., Aleman, A., 2000. Tectonic evolution of the Andes. In: Cordani, U., et al. (Ed.), Tectonic Evolution of South America. 31st Int. Geol. Cong., Rio de Janeiro, Brazil, pp. 453–480.
Raymond, C., Stock, J., Cande, S., 2000. Fast Paleogene motion of the Pacific hotspots from revised global plate circuit constraints. In: Richards, M.A., Gordon, R.G., van der Hilst, R.D. (Eds.), The history and dynamics of global plate motions: AGU Geophys. Monog. Ser., 121, pp. 359–375.
Royer, J.-Y., Chang, T., 1991. Evidence for relative motions between the Indian and Australian plates during the last 20 m.y. from plate tectonic reconstructions: implications for the deformation of the Indo-Australian plate. J. Geophys. Res. 96, 11779–11802.
Royer, J.-Y., Gordon, R.G., Horner-Johnson, B.C., 2006. Motion of Nubia relative to Antarctica since 11 Ma: implications for Nubia–Somalia, Pacific-North America, and India Eurasia motion. Geology 34, 501–504.
Sager, W.W., 2006. Cretaceous paleomagnetic apparent polar wander path for the Pacific plate calculated from Deep Sea Drilling Project and Ocean Drilling Program basalt cores. Phys. Earth Planet. Inter. 156, 329–349.
Sandwell, D.T., Smith, W.H.F., 2009. Global marine gravity from retracked Geosat and ERS-1 altimetry: ridge segmentation versus spreading rate. J. Geophys. Res. 114, B01411. doi:10.1029/2008JB006008.
Schellart, W.P., 2008. Overriding plate shortening and extension above subduction zones: a parametric study to explain formation of the Andes Mountains. Geol. Soc. Am. Bull. 120, 1441–1454.
Sdrolias, M., Dietmar Müller, R., 2006. Controls on back-arc basin formation. Geochem. Geophys. Geosyst. 7 (4), Q04016. doi:10.1029/2005GC001090.
Shaw, P.R., Cande, S.C., 1990. High-resolution inversion for South Atlantic plate kinematics using joint altimeter and magnetic anomaly data. J. Geophys. Res. 95, 2625–2644.
Silver, P.G., Russo, R.M., Lithgow-Bertelloni, C., 1998. Coupling of South America and African plate motion and plate deformation. Science 279, 60–63.
Sleep, N.H., 2006. Mantle plumes from top to bottom. Earth Sci. Rev. 77, 231–271.
Sobolev, S.V., Babeyko, A.Y., 2005. What drives orogeny in the Central Andes? Geology 33, 617–620.
Somoza, R., 1998. Updated Nazca (Farallon)–South America relative motions during the last 40 My: implications for mountain building in the Central Andean region. J. South Am. Earth Sci. 11, 211–215.
Somoza, R., 2005. Cenozoic convergence in western South America: the subduction of the Nazca, Farallon and Phoenix plates. In: Universitat de Barcelona, IRD (Eds.), 6th ISAG, Paris, France, pp. 681–684.
Somoza, R., Ghidella, M.E., 2005. Convergencia en el margen occidental de América del Sur durante el Cenozoico: subducción de las placas de Nazca, Farallon y Phoenix. Rev. Asoc. Geol. Argent. 60, 797–809.
Somoza, R., Zaffarana, C.B., 2008. Mid-Cretaceous polar standstill of South America, motion of the Atlantic hotspots and the birth of the Andean cordillera. Earth Planet. Sci. Lett. 271, 267–277.
Steinberger, B., O'Connell, R.J., 1998. Advection of plumes in mantle flow: implications for hotspot motion, mantle viscosity and plume distribution. Geophys. J. Int. 132, 412–434.
Steinberger, B., Sutherland, R., O'Connell, R., 2004. Prediction of Emperor–Hawaii seamount locations from revised model of global plate motion and mantle flow. Nature 430, 167–173.
Steinerger, B., 2000. Plumes in a convecting mantle: models and observations for individual hotspots. J. Geophys. Res. 105, 11127–11252.
Tarduno, J.A., Cottrell, R.D., 1997. Paleomagnetic evidence for motion of the Hawaiian hotspot during formation of the Emperor seamounts. Earth Planet. Sci. Lett. 153, 171–180.
Tarduno, J.A., Duncan, R.A., Scholl, D.W., Cottrell, R.D., Steinberger, B., Thordarson, T., Kerr, B.C., Neal, C.R., Torii, M., Carvallo, C., 2003. The Emperor Seamounts: southward motion of the Hawaiian hotspot plume in Earth's mantle. Science 301, 1064–1069.
Tassara, A., Götze, H.J., Schmidt, S., Hackney, R., 2006. Three-dimensional density model of the Nazca plate and the Andean continental margin. J. Geophys. Res. 111, B09404. doi:10.1029/2005JB003976.
Tebbens, S.F., Cande, S.C., 1997. Southeast Pacific tectonic evolution from early Oligocene to Present. J. Geophys. Res. 102, 12061–12084.
Torsvik, T.H., Dietmar Müller, R., Van de Voo, R., Steinberger, B., Gaina, C., 2008. Global plate motion frames: toward a unified model. Rev. Geophys. 46 (RG3004/2008, Paper number 2007RG000227).
Wessel, P., Kroenke, L.W., 2008. Pacific absolute plate motion since 145 Ma: an assessment of the fixed hot spot hypothesis. J. Geophys. Res. 113, B06101. doi:10.1029/2007JB005499.
Wilson, J.T., 1963. A possible origin of the Hawaiian Islands. Can. J. Phys. 41, 863–870.
Yañez, G., Cembrano, J., 2004. Role of viscous coupling in the late Tertiary Andean tectonics. J. Geophys. Res. 109, B02407. doi:10.1029/2003JB002494.

Supplementary Data

1) Finite reconstructions – plate circuit

Chron	Age	rotations
C3n.3n (o)	4.9	A+H+K
C5n.2n (o)	10.8	A+H+K
C5C.1n (y)	16.0	A+H+K
C6n (o)	20.2	B+D+H+K
C8n.1n (y)	25.8	B+D+H+K
C10n.1n (y)	28.3	B+D+H+K
C13n (m)	33.3	C+D+G+I+K
C18n.2n (y)	39.6	C+D+G+I+K
C21n (m)	47.0	C+D+G+I+K
C25n (m)	56.1	C+D+G+I+K
C31n (y)	67.7	C+D+G+J+K
C32n.1n (m)	71.2	C+D+G+J+K

ROTATIONS

Nazca to Antarctica

Chron	Age	Lat. (°N)	Long. (°E)	angle	source
C3n.3n (o)	4.9	48.23	260.25	- 2.81	A
C5n.2n (o)	10.8	52.66	260.58	- 7.26	A
C5C.1n (y)	16.0	53.01	260.61	- 11.1	A

Farallon to Pacific

Chron	Age	Lat. (°N)	Long. (°E)	angle	source
C6n (o)	20.2	62.38	266.98	-31.01	B
C7 (y)	24.8	63.88	265.25	-38.81	B
C10n.1n (y)	28.3	67.34	259.92	- 43.44	B
C13n (m)	33.3	69.85	253.87	- 49.54	C
C18n.2n (y)	39.6	73.13	245.92	- 56.86	C
C21n (m)	47.0	74.76	237.64	- 64.98	C

C25n (m)	56.1	78.94	223.39	- 71.40	C
C31n (y)	67.7	80.16	208.74	- 77.87	C
C32n.1n (m)	71.2	80.43	204.19	- 80.04	C

Pacific to West Antarctica

Chron	Age	Lat. (°N)	Long. (°E)	angle	source
C6n (o)	20.2	74.00	289.84	16.73	D
C7 (y)	24.8	74.51	290.34	19.92	D
C10n.1n (y)	28.3	74.41	290.5	22.57	D
C13n (m)	33.3	74.44	295.26	27.17	D
C18n.2n (y)	39.6	74.87	305.54	32.19	D
C21n (m)	47.0	74.52	309.81	37.00	E
C25n (m)	56.1	72.76	306.22	41.79	E
C31n (y)	67.7	69.33	306.56	51.05	E
C32n.1n (m)	71.2	68.51	308.14	54.51	F

West Antarctica to East Antarctica

Chron	Age	Lat. (°N)	Long. (°E)	angle	source
C13n (m)	33.3	18.15	162.15	- 0.66	G
C18n.2n (y)	39.6	18.15	162.15	- 1.30	G
C21n (m)	47.0	18.15	162.15	- 1.70	G
C25n (m)	56.1	18.15	162.15	- 1.70	G
C31n (y)	67.7	18.15	162.15	- 1.70	G
C32n.1n (m)	71.2	18.15	162.15	- 1.70	G

East Antartica to Africa

Chron	Age	Lat. (°N)	Long. (°E)	angle	source
C3n.3n (o)	4.9	8.2	310.60	0.69	H
C5n.2n (o)	10.8	8.2	310.60	1.53	H
C5C.1n (y)	16.0	9.95	311.65	2.23	H
C6n (o)	20.2	10.7	312.10	2.78	H
C7 (y)	25.8	12.69	311.84	3.74	H

C10n.1n (y)	28.3	11.69	311.72	4.45	H
C13n (m)	33.3	12.69	315.39	5.64	I_a
C18n.2n (y)	39.6	13.80	316.25	6.96	I_a
C21n (m)	47.0	11.27	318.45	8.61	I_b
C25n (m)	56.1	9.86	314.76	10.53	I_b
C31n (y)	67.7	2.22	319.26	12.50	J
C32n.1n (m)	71.2	1.70	318.78	13.49	J

Africa to South America

Chron	Age	Lat. (°N)	Long. (°E)	angle	source
C3n.3n (o)	4.9	62.05	319.41	-1.61	K
C5n.2n (o)	10.8	62.05	319.41	-3.54	K
C5C.1n (y)	16.0	59.35	322.15	-5.8	K
C6n (o)	20.2	58.77	322.68	-7.49	K
C7 (y)	25.8	57.59	323.73	-9.57	K
C10n.1n (y)	28.3	57.00	324.84	-11.14	K
C13n (m)	33.3	56.17	326.36	-13.49	K
C18n.2n (y)	39.6	57.10	327.00	-16.41	K
C21n (m)	47.0	56.95	328.85	-19.44	K
C25n (m)	56.1	61.35	327.79	-22.27	K
C31n (y)	67.7	63.88	326.39	-25.54	K
C32n.1n (m)	71.2	63.41	326.62	-26.57	K

Sources:

A: Tebbens and Cande (1997); B: Pardo Casas and Molnar (1987), C: Corrêa Rosa and Molnar (1988); D: Croon et al. (2008); E: Cande et al. (1995), F: S.C. Cande (in Müller et al., 2000); G: Cande et al. (2000); H: Royer and Chang (1991), I: Cande et al. (2010; a= dataset 1, b= dataset 2), J: Molnar et al. (1988); K: Müller et al. (1999)

Note:

For the present study we adopted the Farallon to Pacific anomaly 7 reconstruction of Pardo Casas and Molnar (1987) because no error is available for the anomaly 8 reconstruction of Tebbens and Cande (1997), which we used in our previous contributions (Somoza, 1998; Somoza and Ghidella, 2005). As in previous contributions, the older Nazca to Pacific reconstruction in the present study is derived from the anomaly 6m (19.6 Ma) rotation of Pardo Casas and

Molnar (1987) because availability of error estimates, although it is worth noting that, due to the scarcity or absolutely lack of conjugate pairs of crossings of anomaly 6 within individual Pacific-Nazca spreading corridors, Pardo Casas and Molnar (1987) determined his anomaly 6m rotation by interpolation between their anomaly 7 reconstruction and their 10 Ma Pacific-Nazca rotation derived from present-day plate motion (see last part of Section 2 in the main text). Using this interpolated reconstruction, however, does not affect the reliability of the results (see discussion about anomaly 6By reconstruction between Pacific and Nazca, Section 3 of main text).

2) Nazca (Farallon) – South America convergence parameters from 7°S to 42°S

The tables below show the mean convergence rate (*v, cm/yr*) and mean convergence azimuth (*Az., °E*) for each interval as seen in eight sites close to the Peru-Chile trench. The azimuths indicate the motion of the oceanic plate towards South America. Values from intervals marked with asterisks may be not accurate (see main text). Care must be taken when using the parameters from the older intervals to analyze the tectonics in the Andes of Colombia and Ecuador because the possibility of late accretionary events (collision of either oceanic plateau or marginal basin) in those times (i.e. no Andean-type tectonics). Analytical values predicting divergence were omitted (-), although it may be true that Farallon diverged from South America in those times, our suggestion is the presence of an intervening plate converging with the continent (see main text for discussion). Note that ages are rounded.

Interval	3ºN, 282ºE		7ºS, 278ºE		12ºS, 280ºE		17ºS, 285ºE		22ºS, 289ºE	
(Ma)	*v*	*Az.*	*v*	*Az.*	*v*	*Az.*	*v*	*Az.*	*v*	*Az.*
5-0	7.7	80.1	8.3	82.8	8.5	82	8.7	82.8	8.8	78.1
11-5	11.8	81.1	10.5	83.3	10.7	82.6	10.9	83.3	10.9	79.3
16-11	10.0	85.2	10.8	87.6	11.1	86.7	11.4	87.5	11.5	82.4
20-16	9.7	73.1	11.1	79	11.9	78	12.6	74.1	13.2	71.8
24-20	13.5	84.9	14.3	86.5	14.5	85.9	14.6	86.5	14.6	83
33-28	9.5	59.9	9.2	56.6	8.7	55.7	8.1	56.6	7.3	53.8
40-33	10.6	63	10.2	60	9.7	59.3	9	60	8.2	57.8
47-40	10.2	65.4	9.8	63.1	9.4	62.5	8.8	63.1	8.1	61.8
56-47*	8.7	92.3	6.9	87.2	5.9	90	5	99.7	4.2	111
68-56*	-	-	4.9	25.5	4.4	16.3	3.5	25.9	2.8	353.2

Interval	27ºS, 288ºE		32ºS, 287ºE		37ºS, 285ºE		42S, 285ºE		49S, 284ºE	
(Ma)	*v*	*Az.*	*v*	*Az.*	*v*	*Az.*	*v*	*Az.*	*v*	*Az.*
5-0	8.8	78.6	8.7	78.9	8.6	79.7	8.5	79.7	-	-
11-5	10.9	79.3	10.8	79.6	10.6	80.2	10.4	80	-	-
16-11	11.5	82.8	11.4	83.2	11.3	84	11.1	84.3	10.6	84.6
20-16	13.5	73	13.8	74	14	75.6	14.1	75.7	14	77
24-20	14.4	82.9	14.2	83.1	13.9	83.6	13.4	83.4	12.6	76.7
33-28	6.9	50.3	6.5	46.3	6.2	41.4	5.7	35.9	5.2	26.7
40-33	7.7	54.7	7.2	51	6.8	46.4	6.2	42.2	5.6	33.4
47-40	7.6	58.8	7.2	55.8	6.7	52.1	6.2	48	5.5	41.5
56-47*	3.1	115	2.1	123.3	1	141	-	-	-	-
68-56*	-	-	-	-	-	-	-	-	-	-

3) Stage 1 – Comparison of convergence rate using the Nazca-Antarctica rotations for the 16-0 Ma time span (this paper) with an alternative circuit following the Nazca-Pacific + Pacific-Antarctica rotations

The figure below shows the convergence rate curves for Stage 1 as seen at 22°S for: 1) this paper (red) using the Nazca-Antarctica rotations of Tebbens and Cande (1997) for the 16-0 Ma interval; 2) Mayes et al. (1990) (blue) using their Nazca to Pacific rotations for the Neogene; 3) Wilder (2003) (green) using his Nazca to Pacific rotations for the Neogene. In the two latter cases the circuit was completed with the Pacific to Antarctica rotations of Croon et al. (2008). Numbers below the curves are mean convergence azimuth for each interval of Mayes et al. (1990) and Wilder (2003) (each with the respective color). Although the ages of reconstructions are different, the general tendency to a Late Cenozoic slowdown in observed in all the cases.

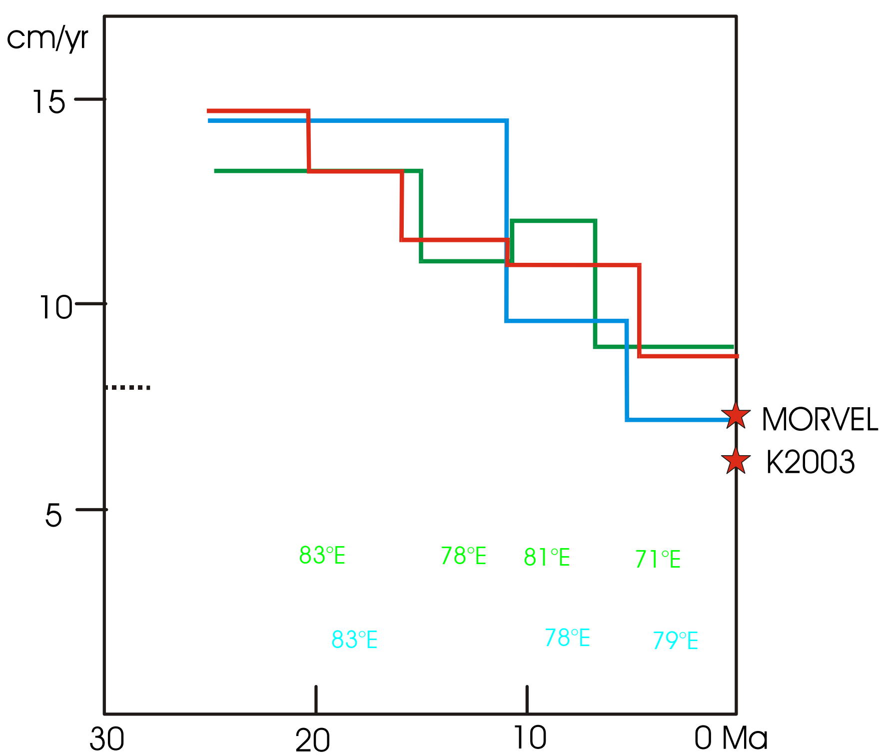

References:

Cande, S. C., Raymond, C., Stock, J., and Haxby, W, 1995. Geophysics of the Pitman Fracture Zone and Pacific Antarctica plate motions during the Cenozoic. Science 270, 947-953.

Cande, S. C., Stock, J. M., Dietmar Müller, R., and Ishihara, T., 2000. Cenozoic motion between East and West Antarctica. Nature 404, 145-150.

Cande, S.C., Patriat, P., Dyment, J., 2010. Motion between the Indian, Antarctic and African plates in the Early Cenozoic. Geophys. J. Int. 183, 127-149

Corrêa Rosa, J. W., and Molnar, P., 1988. Uncertainties in reconstructions of the Pacific, Farallon, Vancouver, and Kula plates and constraints on the rigidity of the Pacific and Farallon (Vancouver) plates between 72 and 35 Ma. J. Geophys. Res. 93, 2997-3008.

Croon, M.B., Cande, S.C., Stock, J.M., 2008. Revised Pacific-Antarctic plate motions and geophysics of the Menard fracture zone. Geochem. Geophys. Geosyst. 9, doi:10.1029/2008GC002019

Mayes, C.L., Lawver, L.A., Sandwell, D.T., 1990. Tectonic history and new isochron chart of the South Pacific. J. Geophys. Res. 95, 8543-8567

Molnar, P., Pardo Casas, F., Stock, J., 1988. Uncertainties in the reconstruction of the Indian, African, and Antartic plates since Late Cretaceous time. Basin Res. 1, 23-40

Müller, R.D., Cande, S.C., Roger, J-Y, Roest, W.R., Machenkov, S., 1999. New constraints on the Late Cretaceous/Tertiary plate tectonic evolution of the Caribbean, in: Mann, P. (Ed.), Sedimentary Basins of the World, 4, Caribbean Basin, Elsevier, New York, pp. 39-55

Müller, R. D.; C. Gaina; A. Tikku; D. Mihut; S.C. Cande and J.M. Stock; 2000. Mesozoic/Cenozoic tectonic events around Australia; In: Richards et al. (Eds.), The History and Dynamics of Global Plate Motions. AGU Geophys. Mon. Ser. 121, pp. 161-188

Pardo Casas, F., Molnar, P., 1987. Relative motion of the Nazca (farallon) and South American plates since Late Cretaceous. Tectonics 6, 233-248

Royer, J.-Y., Chang, T., 1991. Evidence for relative motions between the Indian and Australian plates during the last 20 m.y. from plate tectonic reconstructions: Implications for the deformation of the Indo-Australian plate. J. Geophys. Res. 96, 11779-11802

Tebbens, S.F. and S.C. Cande; 1997. Southeast Pacific tectonic evolution from early Oligocene to Present. J. Geophys. Res. 102, 12061-12084

Wider, D.T., 2003. Relative motion history of the Pacific-Nazca (Farallon) plates since 30 million years ago. Ms. Thesis, University of South Florida, 94 pp.